Universiteit Antwerpen

This item is the archived peer-reviewed author-version of:

A packed-bed DBD micro plasma reactor for CO_2 dissociation : does size matter?

Reference:
Uytdenhouw en Yannick, Van Alphen Senne, Michielsen Inne, Meynen Vera, Cool Pegie, Bogaerts Annemie.- A packed-bed DBD micro plasma reactor for CO_2 dissociation : does size matter?
Chemical engineering journal - ISSN 1385-8947 - 348(2018), p. 557-568
Full text (Publisher's DOI): https://doi.org/10.1016/J.CEJ.2018.04.210
To cite this reference: https://hdl.handle.net/10067/1512380151162165141

uantwerpen.be
Institutional repository IRUA

A packed-bed DBD micro plasma reactor for CO_2 dissociation: Does size matter?

Y. Uytdenhouwen [a,b,*], S. Van Alphen [a], I. Michielsen [a,b], V. Meynen [b], P. Cool [b], A. Bogaerts [a]

[a] Research Group PLASMANT, Department of Chemistry, University of Antwerp, Universiteitsplein 1, Wilrijk B-2610, Belgium

[b] Research Group LADCA, Department of Chemistry, University of Antwerp, Universiteitsplein 1, Wilrijk B-2610, Belgium

*Corresponding author:
Yannick Uytdenhouwen
Universiteitsplein 1, B2.28
Wilrijk B-2610, Belgium
+3232652369
yannick.uytdenhouwen@uantwerpen.be

Highlights:

- Submillimetre discharge gap sizes greatly increase the CO_2 conversion.
- Packing materials can further increase the CO_2 conversion.
- Results greatly dependant on used material, gap and sphere size combination.
- Maximum conversions of 50-55 % obtained for certain combinations and flow rates.
- Maximum energy efficiency of 4.3 % at empty reactor and high flow rates.

Keywords:
Plasma; Dielectric barrier discharge; CO2 dissociation; Micro gap reactor; Packed-bed reactor; Electrical characterization

Abbreviations:
DBD, Dielectric Barrier Discharge; VOC, Volatile Organic Compounds; SS, Stainless Steel; HV, High Voltage; MFC, Mass Flow Controller; LV, Low Voltage; YSZ, Yttria-Stabilized Zirconia; VITO, Flemish Institute for Technological Research; GC, Gas Chromatograph; FID, Flame Ionization Detector; TCD, Thermal Conductivity Detector; X_{GC}, Conversion calculated based on GC data; $[CO_{2,in}]$, Concentration of CO_2 measured by GC without plasma; $[CO_{2,out}]$, Concentration of CO_2 measured by GC after plasma treatment; X_{CO2}, Actual CO_2 conversion based on X_{GC} corrected for gas expansion; $\Delta H_{R,}$ The reaction enthalpy of CO_2 dissociation; SEI, Specific Energy Input; η, Energy efficiency; $\dot{V}$, Volumetric flow rate; P, Plasma power; V_m, The molar gas volume; SI, Supplementary information; U, Voltage; I, Current; Q, Charge; U_{pp}, Peak-to-peak voltage; I_{RMS}, Root-mean-square current; T, Period length; Q_{disp}, Displaced charge; C_{cell}, Capacitance of the reactor without the presence of plasma; C_{diel}, Capacitance of the reactor (=dielectric layer) after full plasma discharge; ζ_{diel}, Effective capacitance of the reactor at partial plasma discharge; α, Partial discharged fraction of the reactor; C_{gap}, Capacitance of the gas filled gap; β, Partial undischarged fraction of the reactor; Δ_U, Voltage difference between DA and BC in the Lissajous figure at Q=0; U_{bur}, Burning voltage; S_n, Sample standard deviation of the measurements; n, sample size; T_s, The two-tailed inverse of the Student t-distribution; p, Probability interval; r_d, Dissociation rate; E_y, Energy yield; ε, dielectric constant / relative permittivity;

Abstract

DBD plasma reactors are of great interest for environmental and energy applications, such as CO_2 conversion, but they suffer from limited conversion and especially energy efficiency. The introduction of packing materials has been a popular subject of investigation in order to increase the reactor performance. Reducing the discharge gap of the reactor below one millimetre can enhance the plasma performance as well. In this work, we combine both effects and use a packed-bed DBD micro plasma reactor to investigate the influence of gap size reduction, in combination with a packing material, on the conversion and efficiency of CO_2 dissociation. Packing materials used in this work were SiO_2, ZrO_2, and Al_2O_3 spheres as well as glass wool. The results are compared to a regular size reactor as a benchmark. Reducing the discharge gap can greatly increase the CO_2 conversion, although at a lower energy efficiency. Adding a packing material further increases the conversion when keeping a constant residence time, but is greatly dependent on the material composition, gap and sphere size used. Maximum conversions of 50-55 % are obtained for very long residence times (30 s and higher) in an empty reactor or with certain packing material combinations, suggesting a balance in CO_2 dissociation and recombination reactions. The maximum energy efficiency achieved is 4.3 %, but this is for the regular sized reactor at a short residence time (7.5 s). Electrical characterization is performed to reveal some trends in the electrical behaviour of the plasma upon reduction of the discharge gap and addition of a packing material.

1 Introduction

Plasma reactors are widely used for both research and industrial purposes [1–5]. Applications vary from treatment of solids and liquids, to decomposition of pollutants such as VOC's and NO_x, and the synthesis of molecules like ozone and (oxygenated) hydrocarbons. There exist various types of plasma reactors, such as microwave discharges, corona discharges, gliding arc discharges, glow discharges, and radio frequency discharges; all with their own advantages and drawbacks [6]. A popular type of reactor for many years is the dielectric barrier discharge (DBD) reactor, because it is easy to operate at conditions of elevated pressure (up to several bar) and near room temperature, and it has a simple,

robust, and easily up scalable design [4]. It is since long the preferred type for big scale ozone generation, but is more recently also applied for surface treatments in the form of a plasma jet and in decomposition and conversion of greenhouse gasses into value added chemicals [5].

The main drawbacks of the DBD reactor up till now are its poor conversion and energy efficiency. In the case of VOC decomposition, removal values of around 60-80 % are obtained for benzene (up to 99 % depending on the applied conditions), 20-70 % for toluene, and even values of over 99 % were reported for trichloroethylene [7]. This is, however, accompanied by a large energy demand, i.e., up to above thousands of J/L for the harder to remove compounds and low pollutant concentrations (100-1000 ppm). For the synthesis of value added chemicals from waste stocks, like greenhouse gas conversion, generally lower conversion values are reached. For instance, dry reforming of methane experiments performed by Tu and Whitehead reached only a maximum CH_4 conversion of 50 % with a corresponding efficiency of only 0.10 mmol/kJ [8]. The highest efficiency they obtained was 0.19 mmol/kJ at a CH_4 conversion of only 15 %.

The values obtained up to now in DBD reactors are not yet sufficient to implement them as a single technology in industrial applications without any further improvement. A first widely used approach for improvement is the implementation of a (catalytic) packing material in the reaction volume of the reactor, to create a so-called packed bed reactor. By adding a packing material to the reaction volume, the plasma behaviour and related chemistry will be altered. A packing material can lead to electric field enhancement [9] by polarization and surface roughness of the particles, as well as changing the discharge type, forming micro plasmas in pores [10], and altering the chemistry by (catalytic) surface reactions [11,12]. Commonly, spheres or other shaped particles of different materials are applied [1,7,8,13–17], due to their easy implementation in the reactor, possibility for catalytic activation, large number of contact points, and wide commercial availability for numerous materials. In addition, wool-type materials like glass wool for their high surface area, or ceramic foams for their rigid 3D structure [13,14,18,19], have also been used. Numerous publications show that adding packing materials to the

DBD reactor can indeed, depending on the applied material-set-up combination, enhance the conversion and efficiency [2,7,8,15,17,20]. The decomposition of e.g. toluene found enhanced removal values of 40-96 % and energy demands could be lowered to values of a few hundred J/L [7]. In the case of dry reforming of methane, an increase of CH_4 conversion was found from 30 to 56.4 % by adding 10%Ni/γ-Al_2O_3 spheres to the reaction volume for the same conditions, and the efficiency rose from 0.14 to 0.32 mmol/kJ [8]. A comprehensive overview of the state-of-the-art of DBD and other plasma reactor types, both packed and unpacked, for CO_2 conversion and dry reforming of methane, can be found in the recent review paper by Snoeckx and Bogaerts [5], presenting all results obtained up to now in terms of conversion, energy efficiency and energy cost.

Another method of improving the performance of the reactor lies in the design itself. The distance between the reactor electrodes, either one or both covered by a dielectric material, not only defines the reaction volume; it has an important influence on the electrical behaviour of the reactor as well [21]. For a fixed potential applied over the electrodes, the electric field strength generated in the reactor is inversely proportional to the distance between the electrodes. It is therefore speculated that decreasing this distance, and thus increasing the electric field, will result in a more powerful plasma for the same applied potential. Also, confining plasmas at elevated pressures to sub-millimetre dimensions, yielding a so-called micro DBD reactor, is said to stabilize the plasma [22]. Bai et al. [23] suggested that decreasing the inter-electrode distance could increase the conversion and efficiency substantially for ammonia synthesis from methane and nitrogen mixtures. Sekiguchi et al. [24] reported that benzene hydroxylation increased by a factor of 4 when decreasing the inter-electrode distance.

Both of these improvements have been found successful and combining both approaches might even be better. The smaller gap can enhance the overall electric field, while the spheres can further enhance the local electric field between them. This in turn should provide us with a packed bed micro DBD reactor that is expected to even further improve the performance of the original DBD reactor.

The targeted reaction in this work is CO_2 dissociation in CO and O_2. This reaction is preferred for the purpose of this study over bi-component mixtures, like dry reforming of methane, because of its simple chemistry, to provide us with a more fundamental insight in the behaviour of the plasma in the DBD reactor with yet enough chemistry compared to a non-reactive gas, like helium or argon.

Following the hypotheses introduced above, the overall research question can be summarized as: Does size matter? This question will be answered here, split up into three sub questions:

1: What is the influence of gap size reduction in a DBD plasma reactor on the CO_2 conversion, and can the electrical parameters be linked?

2: What is the influence of the size and type of packing materials and can they even further improve the performance of the reactor? Is there a difference depending on the type of material?

3: Will these improvements also translate in higher energy efficiency?

2 Materials and methods

The experimental setup can be divided into three parts: (i) the DBD reactor forming the heart of the setup, which is being controlled by (ii) the gas and (iii) electrical circuit, to steer and analyse the underlying chemistry and electrical behaviour. Analysis of the gas composition after the plasma reaction for calculating the conversion and analysis of the electrics for determining the power are straightforward and common operations, but we will go one step further in analysing the electric signals. Quantifying the discharge performance can show us more detailed information on the underlying behaviour of the plasma in the (packed) micro gaps.

2.1 Experimental set-up

2.1.1 Reactor

The reactor in this work is a cylindrical DBD reactor as shown in Figure 1. The concentric design has the advantage of providing a more uniform reaction volume, since there are no extra boundaries except for the dielectric wall and the electrode, and it is easier to use in both milli and micro gap configuration.

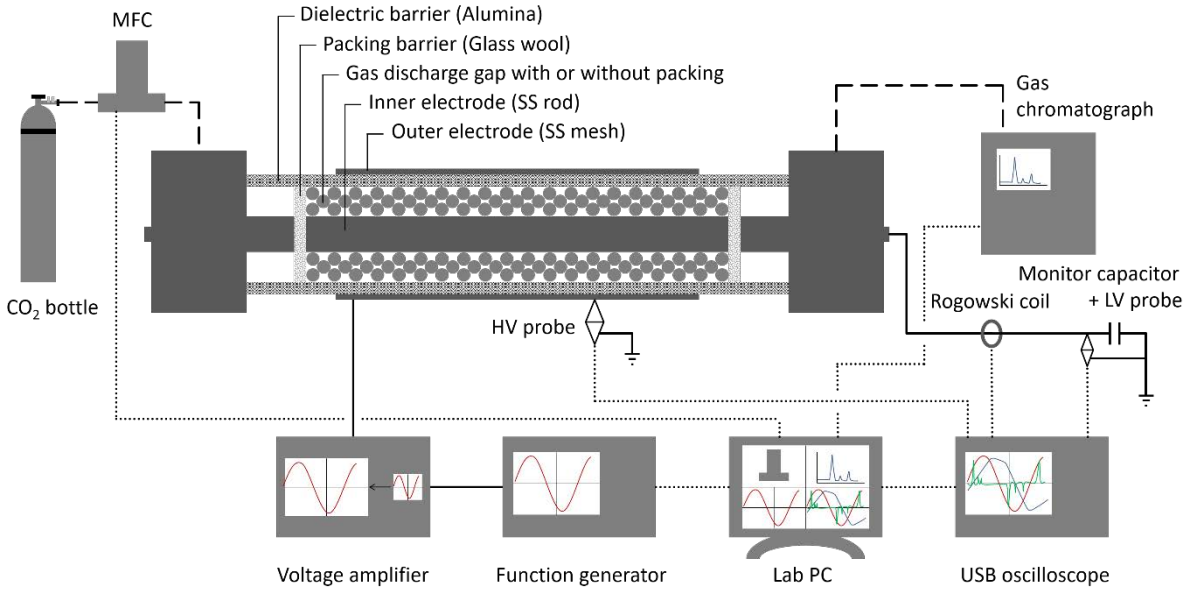

Figure 1: Packed bed DBD reactor used in this work with analytical equipment.

The reactor body is made of an alumina dielectric tube with 22 mm outer diameter and a precision machined inner diameter of 17.41 mm. The live electrode is a stainless-steel mesh with a length of 100 mm that is tightly wound around the dielectric tube to form the outer electrode. A stainless-steel rod is placed in the centre of the tube to be used as the grounded inner electrode, to shape the reaction volume and alter the discharge gap. Five inner electrodes with different outer diameters were used in this research, resulting in discharge gap sizes of 268, 455, 705, 1230, and 4705 µm. The first four gap sizes will be considered as micro gaps in this work and the last one as a milli gap; this is the benchmark that is also used in our other research [14]. Besides using the empty reactor as such, experiments were also performed with different packing materials. Spheres with different compositions made of SiO_2, YSZ (yttria-stabilized zirconia) (both Sigmund Lindner), and α-Al_2O_3 (custom made at VITO) [25] were used in three size ranges: 100-200 µm, 300-400 µm, and 800-900 µm. In addition, glass wool (superfine 8 - 50 µm) (Glaswarenfabrik Karl Hecht) was also used as a packing material.

2.1.2 Gas circuit

The reactor was fed with a pure CO_2 stream that is set and controlled by a mass flow controller (Bronkhorst EL-FLOW Select). Each reactor condition was tested with the same residence time of 7.5 s in order to isolate the influence of modifying the discharge gap size and adding a packing material in

the reactor. Therefore, for an empty reactor, flow rates of 11.52, 19.35, 29.53, 50.00, and 150.18 mL/min were used for the 268, 455, 705, 1230, and 4705 µm gap sizes, respectively. The available reaction volume decreases when adding a packing material, and assuming a close spherical packing, this results in a 74.048 % decrease in available reaction volume. Thus, adjusted lower flow rates were used to match the 7.5 s residence time: 2.99, 5.03, 7.68, 12.98, and 38.98 mL/min. These flow rates were also used for the glass wool filled reactor (i.e. a tightly wound long strip around the centre electrode filling the whole reaction volume), since it is not directly possible to estimate the volume loss of adding this non-uniformly shaped material.

The small flow rates do not have great industrial value but the focus in this work lies in exploring the "isolated" effect of the packing parameters. Furthermore, if higher throughputs are desirable, the influence of raising the flow rate within a specific reactor has been shown numerous times [14,23,26,27] (higher flow rate equals lower conversion); but solutions provided by using larger reaction volumes to get the same residence time, and/or placing multiple reactors in parallel are available [28].

2.2 Performance characterization: conversion and efficiency

The gas stream leaving the reactor was analysed by a gas chromatograph (Trace GC 1310, Interscience). This GC has 12 pressureless sample loops for rapid sampling combined with both a flame ionization detector (FID) and thermal conductivity detector (TCD) channel. Since the products formed in this reaction are CO, O_2, and traces of O_3, besides unreacted CO_2, only the TCD channel was used. The CO_2 conversion derived from the GC data was defined as:

$$X_{GC,y} = \frac{n_{\dot{CO_2}_{in}} - n_{\dot{CO_2}_{out}}}{n_{\dot{CO_2}_{in}}} \qquad (1)$$

with $n_{\dot{CO_2}}$ the molar flow rate of CO_2. This value is, however, not correct in a pressureless sampling system (sampling at atmospheric pressure). As one mole of CO_2 is split into 1 mole of CO and 0.5 mole of O_2, this gives rise to a gas expansion of a factor 1.5 in case of 100 % conversion. Therefore, the

pressure in the reactor, in the tubing leading to the GC, and eventually in the sample loops within the GC, will increase. When the GC samples, it will depressurise the sample loop to atmospheric pressure and thus loses a number of molecules to be detected. This will result in an apparent lower peak area and thus CO_2 concentration, leading to an overestimation of the CO_2 conversion. As a consequence, the overestimated conversion has to be corrected based on the actual gas conversion and expansion. The actual CO_2 conversion (X_{CO_2}) can be calculated by the following equation, shown by Pinhão et al. [29] and Snoeckx et al. [30]:

$$X_{GC} = 1 - \left(\frac{1-X_{CO_2}}{1+\frac{X_{CO_2}}{2}}\right) \Leftrightarrow X_{CO_2} = \frac{2\,X_{GC}}{3-X_{GC}} \qquad (2)$$

The energy efficiency of the conversion can be calculated based on the theoretical required and actual consumed energy. The energy efficiency is therefore defined as:

$$\eta = \frac{\Delta H_r\, X_{CO_2}\, \dot{V}}{P\, V_m} \qquad (3)$$

with ΔH_r the reaction enthalpy of CO_2 dissociation (279.8 kJ/mol), $\dot{V}$ the volumetric flow rate, P the plasma power, and V_m the molar gas volume (22.4 L/mol). The ratio of the plasma power over the volumetric flow rate is also known as the specific energy input or SEI:

$$SEI = \frac{P}{\dot{V}} \qquad (4)$$

2.3 Electrical characterization

The outer electrode of the reactor was driven by a high voltage amplifier (TREK, Model 20/20C-HS) that amplifies an input signal by a factor 2000. This input signal was provided by a PC controlled function generator (Tektronix, AFG 2021) at a fixed frequency of 3000 Hz and an adjustable amplitude, depending on the reactor configuration, to load the reactor with a power of 30 W. The applied voltage was monitored by a high voltage probe (Tektronix, P6015A), the current pulses were measured by a current transformer (Pearson, Model 4100), and the dissipated charge was determined by using a monitor capacitor (10 nF) and a low voltage probe (Picotech, TA150). All signals were captured by a

digital oscilloscope (Picotech, Picoscope 6402D) with which the plasma behaviour was tracked, and the power was continuously calculated to adjust the amplitude of the function generator. This way, a constant plasma power of 30 W was maintained.

Each experiment was evaluated by analysing the signals recorded by the digital oscilloscope: the applied voltage ($U(t)$), the resulting current flow ($I(t)$), and the dissipated charge ($Q(t)$). The resulting oscillogram (cf. Figure 2a) yields the peak-to-peak voltage (U_{pp}), the mean current (I_{RMS}), and the plasma power (P). The latter can be calculated during one or multiple period lengths (nT):

$$P = \frac{1}{nT}\int_0^{nT} U(t)I(t)\,dt \qquad (5)$$

Using the applied voltage and the dissipated charge, we can plot a Q-U graph, also known as a Lissajous figure, schematically illustrated in Figure 2b. Manley [31] has shown that the plasma power can also be determined from the area of the resulting graph:

$$P = \frac{1}{T}\oint U(Q)dQ \qquad (6)$$

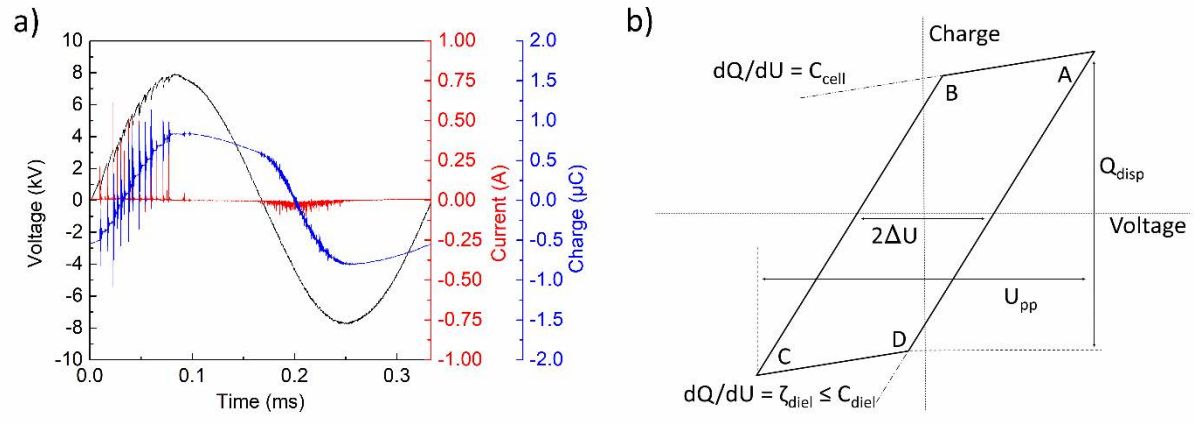

Figure 2: a) Typical data acquired from the digital oscilloscope displayed for one period. b) Simplified Lissajous figure generated by plotting charge as a function of applied voltage, annotated with typical measured values.

Further analysis of the oscillogram and resulting Lissajous figure is done to calculate the peak-to-peak voltage (U_{pp}), root-mean-square current (I_{RMS}), effective capacitance (ζ_{diel}), partial discharging fraction (α), burning voltage (U_{bur}), displaced charge (Q_{disp}), number of micro discharges per period, and displaced charge per micro discharge. Extra information about the extraction of these parameters

and associated theory can be found in the supplementary information. Calculation of all the electrical parameters is done automatically by a MATLAB script.

2.4 Experimental method

A cooled-down (freshly packed) reactor was used for each experiment and operated for 40 min to achieve steady-state conversion, followed by the GC and Lissajous measurements. The input voltage was continuously adjusted to match the desired plasma power of 30 W.

Each experiment was performed three times with four GC and Lissajous analyses for statistical review. The error bars are subsequently defined as:

$$error = \pm S_n \frac{T_s(p,n)}{\sqrt{n}} \qquad (7)$$

with S_n the sample standard deviation of the measurements, n the sample size being 12, and T_s the two-tailed inverse of the Student t-distribution for sample size n and probability p set at 95 %.

3 Results and discussion

In order to answer the research questions listed in the introduction, the results will be judged both on the gas analysis and electrical parameters. The results for the empty reactor will be shown first to partially answer the first question of this work. Subsequently, the results for the packed reactors will be presented to further supplement the former data and to investigate the second question. At the end of each sub-section, the efficiency will be discussed to provide answers to the third question.

3.1 Empty reactor

3.1.1 Conversion

Figure 3 illustrates the influence of the gap size on the CO_2 conversion, for a plasma power of 30 W, both at a constant residence time of 7.5 s and 28.9 s (corresponding to the flow rate of the corresponding packed bed reactors), for gaps typical of both a micro reactor and a regular sized reactor. The conversion increases remarkably by decreasing the gap size, up to 33.3 % and 53.7 %

conversion at the smallest gap, for the residence time of 7.5 s and 28.9 s, respectively. This is an increase with a factor 2.6 and 1.8 compared with the largest micro gap of 1230 µm, and with a factor 7.8 and 4.9 with respect to the regular sized reactor. This trend is logical, because both the reduced electric field strength and the power density rise by reducing the discharge gap size (at constant applied voltage and power).

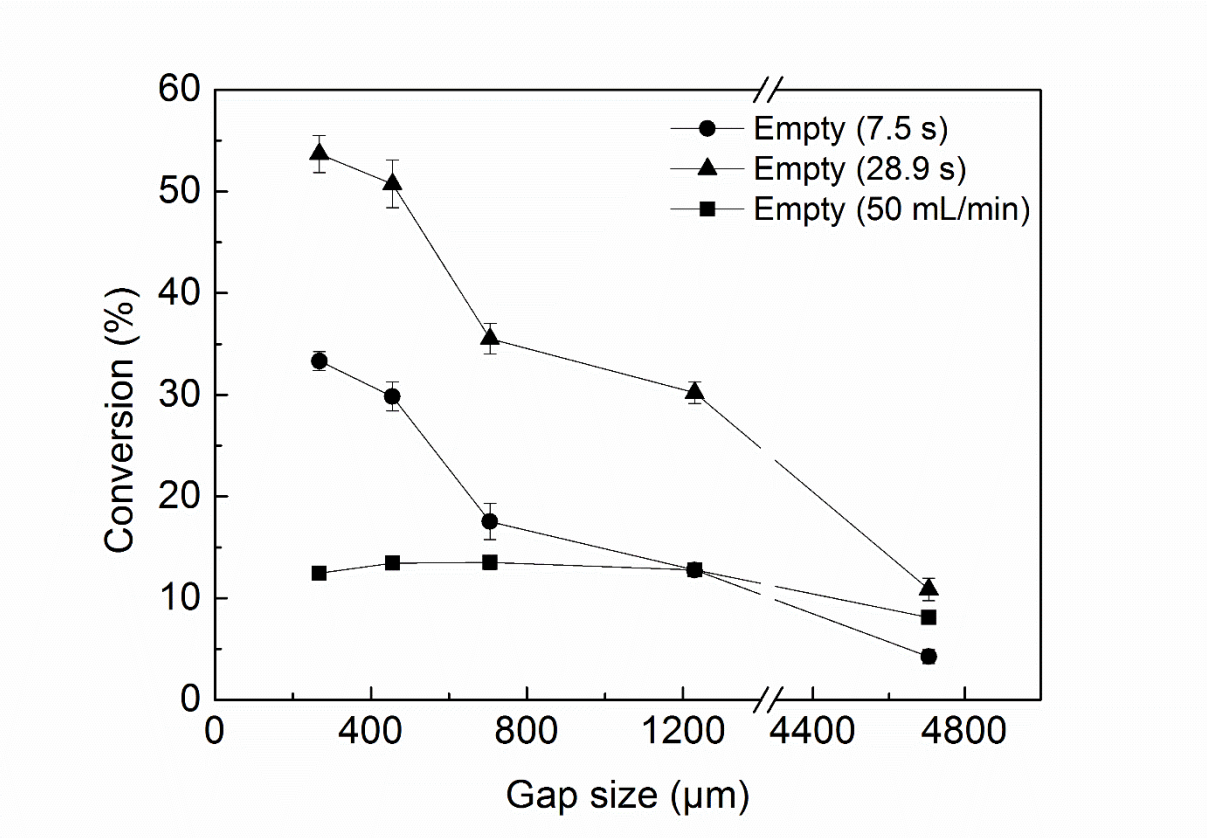

Figure 3: Conversion as a function of gap size for an empty reactor at a constant residence time of 7.5 s and 28.9 s, and at a constant flow rate of 50 mL/min at 30 W plasma power.

When reducing the gap size, the reduced electric field enhances proportionally, from 503 Td at 1230 µm to 2304 Td at 268 µm, leading to a number of effects. First of all, a higher reduced electric field yields a higher electron temperature, resulting in more successful electron impact excitation and ionization reactions, which are the most prominent reactions for CO_2 dissociation in a DBD reactor [32]. In addition, the ionization reactions cause a higher density of electrons and ions, resulting in an overall more reactive plasma [33], hence the higher conversion. Also, the critical value for the local reduced electric field is reached more often due to the overall higher electric field, resulting in a plasma

that is easier to ignite, and this causes more micro discharges per period in the plasma (see section 3.1.2). The latter gives rise to a higher probability for gas molecules to be hit by a micro discharge and thus be converted upon collision in the plasma.

The specific energy input (SEI) increases as well when the discharge gap becomes smaller. This is because of the lower flow rate used to maintain the same residence time. In the case of 7.5 s residence time, the SEI increases from 36.0 to 156.2 kJ/L with decreasing gap size, and at 28.9 s residence time, the SEI increases from 138.7 to 602.0 kJ/L. This higher SEI also creates a more reactive plasma, resulting in a higher conversion. It was not possible to compare the different gap sizes at both a constant SEI and constant residence time, because the corresponding plasma powers could not be applied due to limitations of reactor and set-up. A constant power of 30 W was therefore used.

The effect of the micro gap is even more notable when the results are compared to the normal sized reactor of 4705 µm. A conversion of only 4.1% and 10.9 % is observed here due to the intrinsic lower reduced electric field of 194 Td, and the lower SEI of only 12.0 and 46.2 kJ/L for the 7.5 s and 28.9 s residence time.

An attempt to isolate the influence of gap size from the SEI was done by performing the experiments at a constant flow rate of 50 mL/min. In this way, a constant SEI of 36 kJ/L is maintained and the results are displayed as well in Figure 3. The results show that the conversion almost does not change from 1230 µm to 268 µm. Two effects occur here at the same time. On one hand, the reduced electric field enhances by decreasing the gap size, resulting in a higher conversion. However, since a constant flow rate was used in reactors with decreasing gap size, the residence time decreases significantly by a factor 4.4, i.e., from 7.5 to 1.7 s. This shows that the reduction of the gap size can compensate for the reduced residence time and thus can enhance the performance of the reactor.

A side note has to be made here that SEI is not really a universal 'input-parameter', as shown by Aerts et al. [32]. Both power and flow rate have their distinct influences on the behaviour of the plasma, gas, and reactor behaviour. The power has a great influence on the magnitude of the applied voltage and

resulting current, and thus on the reduced electric field, and subsequently on the number, and magnitude, of micro discharges. On the other hand, the flow rate has an influence on the general reactor residence time, but as well on the discharge filament residence time (i.e. the time that gas molecules spend in filaments) which is in fact the actual location of reaction. Nevertheless, the SEI can be used as a comparison tool, as long as enough of the set-up parameters are kept the same.

3.1.2 Electrical characterization

Electrical characterization of the experiments supports the trends above. Figure 4 shows the Lissajous figures of the different gap sizes for a residence time of 7.5 s. It reveals a significant change in electrical behaviour upon reducing the gap size, seen by the different slopes, heights, and widths of the different parts of the Lissajous figure.

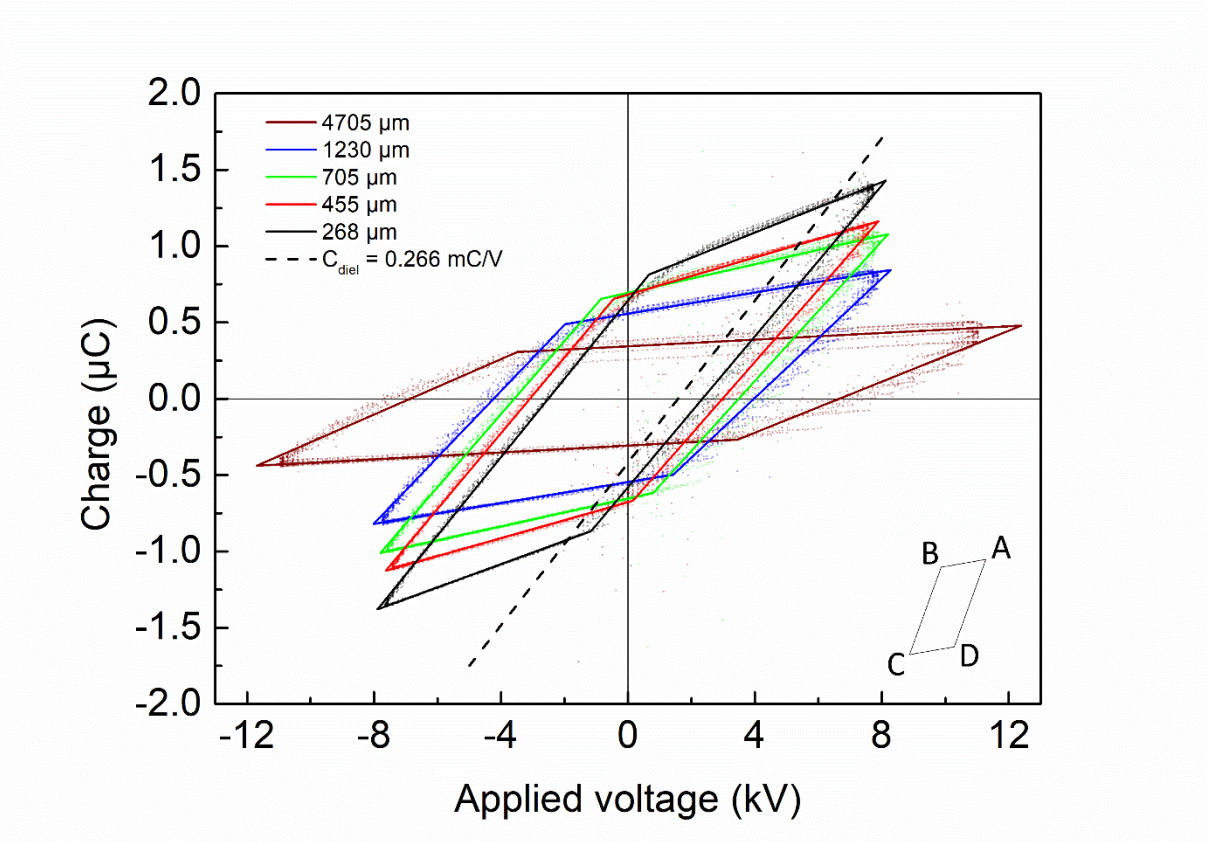

Figure 4: Raw Lissajous plots (dotted) for an empty reactor with different discharge gap sizes for a constant residence time of 7.5 s, as well as the slopes calculated by the MATLAB script (solid lines). Comparison is also made with the C_{diel} value of a completely discharged reactor (dashed line).

First of all, there is a clear change in the slopes of the discharge phase BC and DA (cf. Figure 2 above). The slope, or capacitance, of this phase increases when the discharge gap gets smaller, to approach the capacitance value of a fully discharged reactor, marked by the dashed line. As seen in Table 1, the effective capacitance ζ_{diel} increases from 0.095 to 0.251 mC/V and thus it approaches the value of C_{diel}, i.e., 0.266 mC/V. This means that a smaller discharge gap tends to generate a more uniform (and fully discharged) plasma throughout the whole reaction volume. Indeed, the partial discharging value α (see definition in the SI) drops from 62 % to 7.9 % (see also Table 2). These results match the conversion results, and thus the fact that the more fully discharged reactor is one of the underlying reasons for the higher conversion upon decreasing discharge gap.

Table 1: Measured data from the input signals of the oscilloscope (voltage, current, and charge) and subsequently generated Lissajous figure for the empty reactors with varying gap size at a constant residence time of 7.5 s, calculated by the MATLAB script. The meaning of the parameters is explained in the SI.

Gap size	U_{pp} (kV)	I_{RMS} (mA)	C_{cell} (mC/V)	ζ_{diel} (mC/V)	Transferred charge (µC)	Conversion (%)
268 µm	15.49 ± 0.03	27.9 ± 0.2	0.078 ± 0.001	0.251 ± 0.001	2.2 ± 0.1	33.3 ± 0.9
455 µm	15.25 ± 0.05	28.2 ± 0.5	0.065 ± 0.002	0.246 ± 0.002	1.6 ± 0.2	30 ± 1
705 µm	15.3 ± 0.1	27.8 ± 0.3	0.048 ± 0.001	0.236 ± 0.001	1.57 ± 0.06	18 ± 2
1230 µm	15.5 ± 0.1	28 ± 1	0.034 ± 0.003	0.206 ± 0.003	1.3 ± 0.2	12.8 ± 0.3
4705 µm	23 ± 2	15 ± 2	0.012 ± 0.003	0.095 ± 0.003	0.59 ± 0.06	4.3 ± 0.7

Table 2: Calculated data from the raw data from Table 1 for the empty reactors with varying gap size at a constant residence time of 7.5 s, calculated by the MATLAB script. The meaning of the parameters is explained in the SI.

Gap size	α value (%)	U_{bur} (kV)	Number of micro discharges (a.u./T)	Average filament charge (nC/disch.)	Conversion (%)
268 µm	7.9 ± 0.4	2.605 ± 0.001	49 ± 2	45 ± 2	33.3 ± 0.9
455 µm	10 ± 1	3.21 ± 0.08	29 ± 3	55 ± 3	30 ± 1
705 µm	13.5 ± 0.6	3.737 ± 0.001	26 ± 1	59 ± 2	18 ± 2
1230 µm	26 ± 1	4.375 ± 0.003	24 ± 3	55 ± 5	12.8 ± 0.3
4705 µm	62 ± 2	7.25 ± 0.08	21 ± 2	28 ± 3	4.3 ± 0.7

Secondly, there is a change visible in the voltage difference at $Q = 0$ µC (see Figure 5), which is used further to calculate the burning voltage (U_{bur}). The latter decreases from 7.25 to 2.605 kV upon decreasing discharge gap, as seen in Table 2, making it easier to ignite and sustain the plasma with a lower minimum voltage. The actual applied peak-to-peak voltage to achieve the desired power of 30 W, however, stays about constant at around 15.4 kV, showing a small dip at 455 and 705 µm. This

is significantly lower than the peak-to-peak voltage of 23 kV necessary to achieve a power of 30 W at a discharge gap of 4705 µm. Despite the almost constant peak-to-peak voltage in the micro gaps, a change in the behaviour of the reactor is seen here by the capacitive phases AB and CD, which become shorter and steeper. The latter results from a smaller gap, giving a higher base reactor capacitance. The discharge phases BC and DA, on the other hand, become longer and more powerful. The displaced charge per period increases immensely from 0.59 to 2.2 µC when the discharge gap decreases from 4705 to 268 µm (see Figure 5). This results in a greater part of the applied power that will be available in the plasma, providing a higher chance of high energy discharges and/or more individual discharges, as suggested in section 3.1.1.

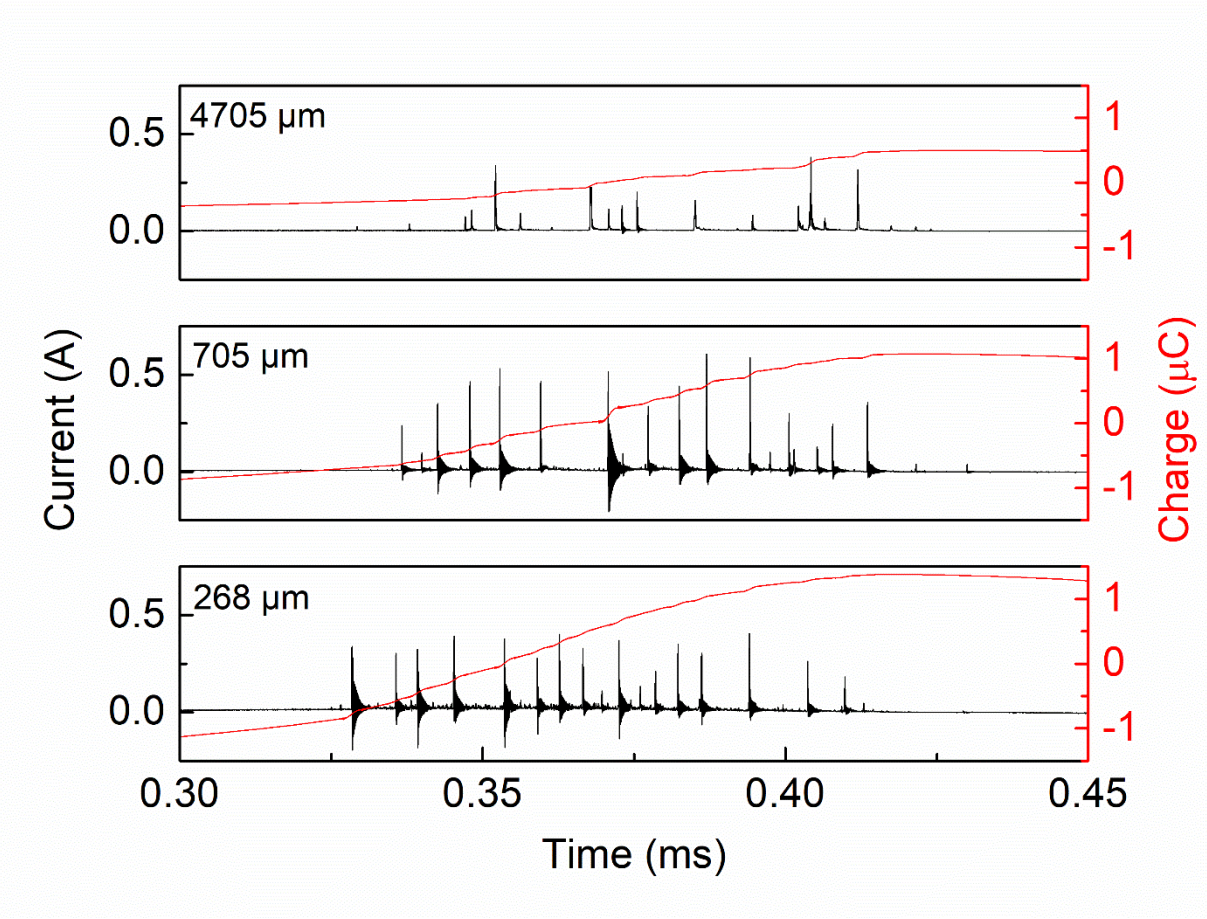

Figure 5: Detailed view of a positive half period of the current and charge profile of a 30 W DBD reactor operating at 4705, 705 and 268 µm discharge gap with a residence time of 7.5 s.

Finally, closer examination of the current profile, as seen in Figure 5, indicates a change in number of micro discharges per period. At a gap size of 4705 µm, only 21 micro discharges on average were

observed per period, while this number increases to 49 in the smallest gap size of 268 µm. This is indeed consistent with the assumption that a higher reduced electric field leads to a higher chance of a discharge propagation in the reactor. The reduced higher electric field, however, does not mean that the micro discharges are more powerful as well. Dividing the number of discharges by the transferred charge shows that the most powerful discharges on average happen at a discharge gap of 705 µm, with an average strength of 59 nC per discharge. The trend goes over a maximum, because the displaced charge during the discharge phase does not increase at the same rate as the number of micro discharges. This suggests that the higher plasma fraction in the discharge volume and the larger number of micro discharges per period have more effect on the CO_2 conversion than the transferred charge.

3.1.3 Efficiency

Although a great conversion is desired, it should be accompanied by a sufficient energy efficiency as well. Therefore, the efficiency will be discussed here, to judge if decreasing the discharge gap, while keeping a constant residence time, is really beneficial.

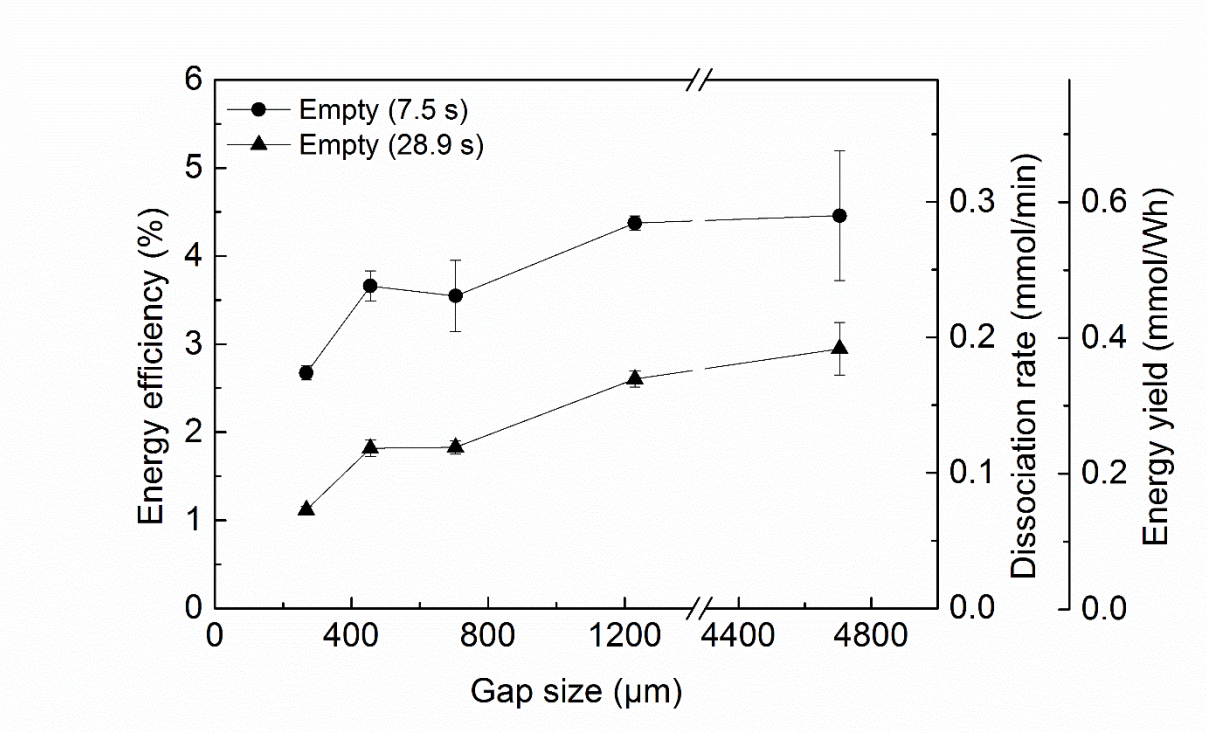

Figure 6: Efficiency as a function of gap size for an empty reactor at a constant residence time of both 7.5 s and 28.9 s. The efficiency is displayed as energy efficiency, as well as dissociation rate and energy yield.

The energy efficiency, displayed in Figure 6, shows the opposite trend from the conversion. Decreasing the discharge gap lowers the energy efficiency for both residence times. Although the conversion is higher at these smaller gap sizes, the energy efficiency also depends on the flow rate (see equation 3 in section 2.2 above), and the latter is lower in the smaller gap sizes to keep the residence time constant. This lower flow rate clearly has a larger overall impact than the enhanced conversion, explaining why the energy efficiency drops upon decreasing gap size. The maximum value of 4.3 % in these experiments was found at the shorter residence time, and thus lower SEI, in the 1230 µm gap size.

The ideal process would have both high conversion and energy efficiency, but this is most of the time not achievable with the particular thermodynamics i.e. the highly endothermic reaction of CO_2 dissociation, as the high thermodynamic stability (high negative Gibbs free energy of formation, ΔG_0) of CO_2 drives the equilibrium strongly to the left. From these results it is evident that there is a trade-off between high conversion and high energy efficiency in this set-up when the discharge gap changes at the same residence time and power input. The quest of finding an optimum in both conversion and energy efficiency comes down to producing as much product per time or per amount of energy, to develop a competitive technology that can eventually be used in industry.

The efficiency can therefore also be expressed as dissociation rate (mmol/min) and energy yield (mmol/Wh), which are related to the energy efficiency, except for a constant factor:

$$\eta = \frac{\Delta H_r}{PV_m} . X_{CO_2}\dot{V}$$
$$r_d = \frac{1}{V_m} . X_{CO_2}\dot{V} \qquad (8)$$
$$E_y = \frac{1}{PV_m} . X_{CO_2}\dot{V}$$

Plotting the results expressed as dissociation rate and energy yield thus shows the same trend as for the energy efficiency; see Figure 6. The maximum values of 0.285 mmol/min and 0.57 mmol/Wh, respectively, are again reached at the shorter residence time at a discharge gap of 1230 µm.

Comparing the results of these three efficiencies with the regular sized gap of 4705 µm shows that increasing the discharge gap yields a somewhat higher efficiency for a residence time of 28.9 s, but the efficiency remains constant for a residence time of 7.5 s. The energy efficiency, dissociation rate and energy yield in the regular sized reactor, under the applied conditions here, are at maximum 4.3%, 0.28 mmol/min and 0.57 mmol/Wh, respectively.

To obtain maximum efficiency, the product of conversion and flow rate should be at maximum when the applied power is constant. Increasing the flow rate, however, will reduce the conversion, because of the shorter residence time. This was checked in an empty reactor with 455 µm discharge gap and fixed power of 30 W, by changing the flow rate from 50 to 2 ml/min, which results in residence times from 2.9 to 72.7 s, as shown in Figure 7.

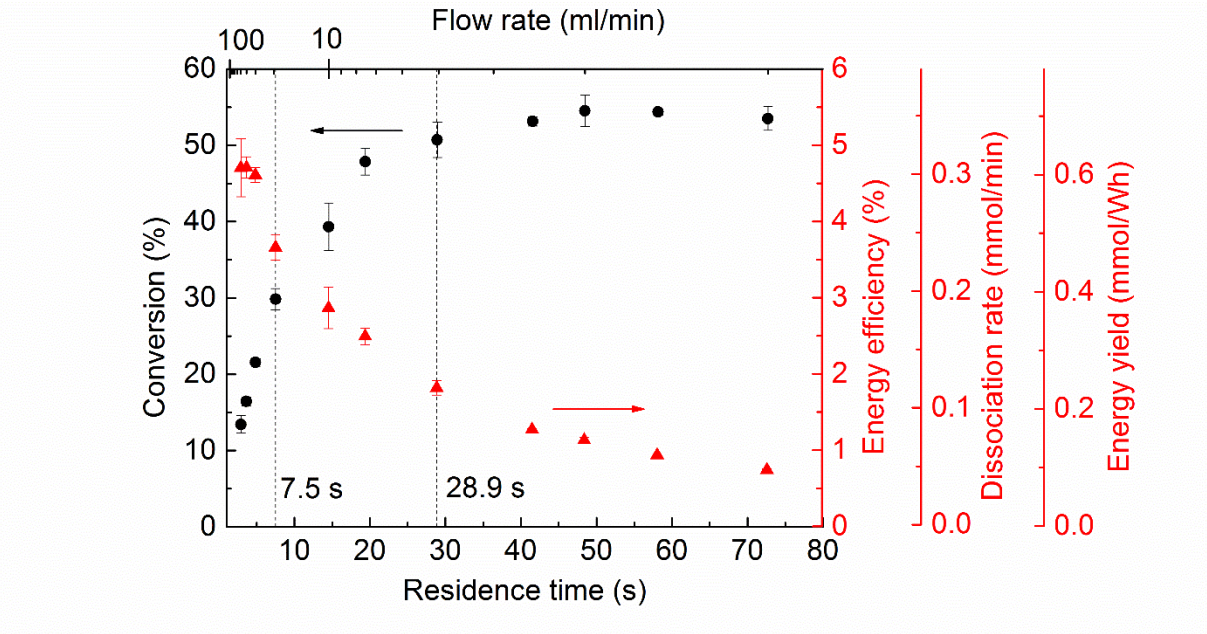

Figure 7: Conversion and efficiency as a function of residence time and flow rate for an empty reactor with gap size of 455 µm. The residence times of 7.5 s and 28.9 s are indicated with vertical dashed lines.

First of all, the results show that, as expected, the steady-state conversion increases with residence time up to 30 s, and then stays more or less constant around 50-55 %. These results demonstrate that a plasma with constant power will need a certain amount of time to convert as much CO_2 as possible. This is due to the filamentary behaviour of the DBD plasma, where a longer residence time means a higher chance of CO_2 molecules to be converted in a micro discharge, resulting in a higher "plasma

residence time". However, the probability for the back reaction will increase as well, and the CO_2 conversion will flatten and reach a plateau when both the forward and backward reactions cancel each other. Further increase in residence after 30 s will only result in further decrease in energy efficiency without any extra conversion. A new plasma-driven equilibrium is reached here, dependent on the reactor set-up conditions, that is different from the traditional thermal equilibrium.

Vice versa, the conversion drops upon higher flow rate, due to the shorter residence time, and this effect eventually is larger than the beneficial effect of higher flow rate on the efficiency. Thus, the product of flow rate and conversion drops. Therefore, the energy efficiency increases with increasing flow rate (and decreasing residence time) up to 20 mL/min, but will then reach a plateau around 4.7 %. The same trend is of course also seen in the dissociation rate and energy yield. Despite the lower conversion, more CO_2 is being dissociated into CO per time and per amount of energy at higher flow rates, reaching values up to 0.3 mmol/min and 0.6 mmol/Wh, respectively.

To further increase the product of conversion and efficiency, the conversion should be increased, without applying higher residence times or higher applied powers. This trade-off can only be surpassed with substantial changes to the reactor parameters, such as pulsed power, or changes to the reactor set-up such as using packing materials, different reactor geometry, discharge type, or CO separation. Improving the energy transfer from the electric field to chemical energy is key in optimizing the overall efficiency of plasma reactors. The next section will discuss the possibility of using packing materials to enhance the performance of DBD (micro gap) reactors.

3.2 Packed reactor

As mentioned in the introduction, implementing a packing material in the reaction zone can have multiple influences to enhance the CO_2 conversion in the plasma. Hence, the combination with a reduced gap size might even further improve the performance of the DBD reactor. Therefore, spheres of three different materials were selected in three different sizes, as well as glass wool. As in the previous section, a constant plasma power of 30 W was kept at 3000 Hz for a residence time of 7.5 s.

3.2.1 Conversion

The CO_2 conversion results of all these experiments are summarized in Figure 8. Note that no data points could be recorded for 100-200 µm ZrO_2 and Al_2O_3 spheres in the smallest gap reactor (268 µm), nor for 300-400 µm Al_2O_3 spheres in the reactor with gap of 455 µm, due to failure of the reactor dielectric. Indeed, sphere-to-gap ratios near 1 are not favourable due to (heat) expansion of the spheres, putting too much stress on the reactor walls.

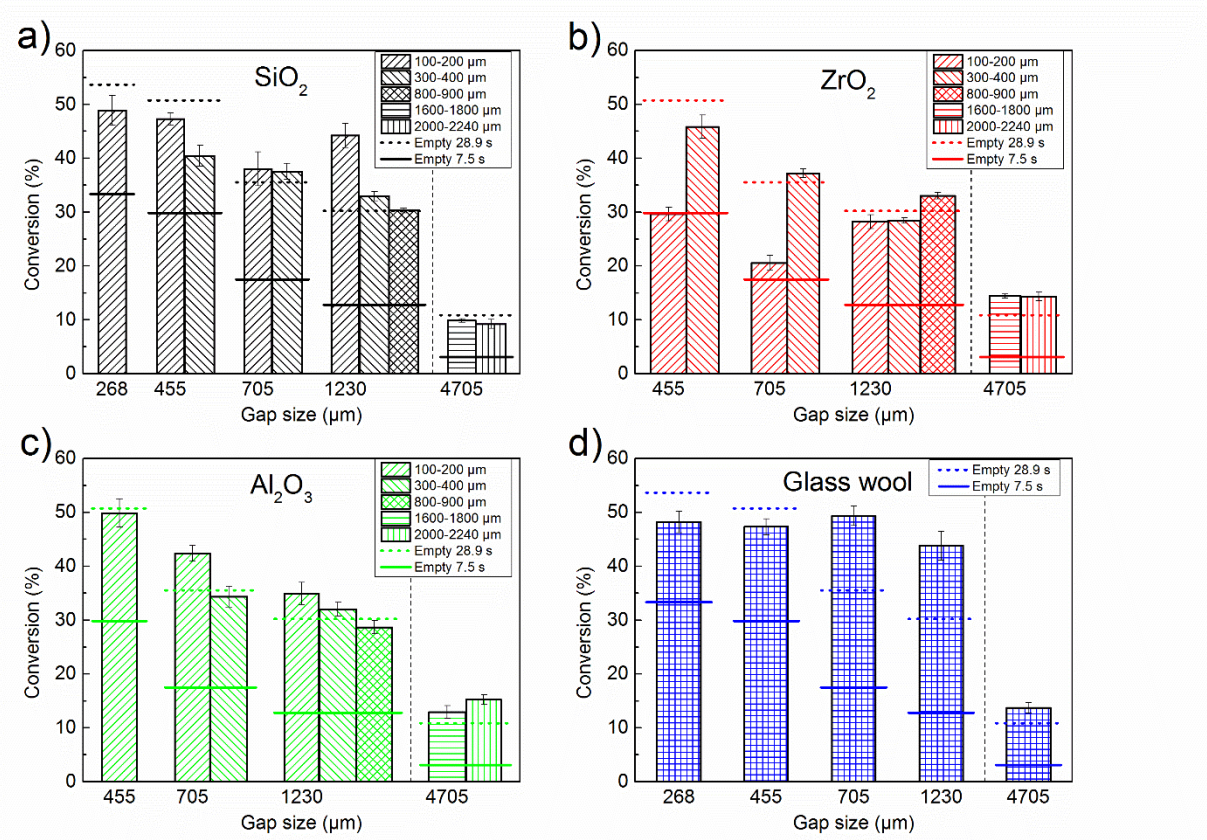

Figure 8: Conversion in packed bed DBD (micro) reactors for a constant residence time of 7.5 s and plasma power of 30 W. The results are displayed per material type for different sphere sizes (indicated by the legend) and as a function of gap size, and compared to the empty reactor at the same residence time of 7.5 s (solid horizontal lines) and a residence time of 28.9 s (corresponding to the same flow rate as the packed bed reactors) (dashed horizontal lines).

A number of interesting trends can be derived from this figure. First of all, adding a packing material significantly enhances the conversion when compared with an empty reactor at the same residence time (see solid horizontal lines). This will partly be due to the enhanced local reduced electric field between the spheres or fibres (in case of glass wool), but also due to the higher power density, because the same power is deposited over a smaller volume due to the presence of the packing. Comparing the

results with the empty reactor of 28.9 s, hence at the same flow rate for a fixed gap, and thus the same SEI, shows however that only some sizes of certain materials can enhance the CO_2 conversion well enough, to compensate for the lower residence time in the packed bed reactors for the same CO_2 throughput. This occurs only in the two largest gap sizes of the micro-reactor, i.e., 705 and 1230 µm, as well as in the regular size reactor. The most noticeable results are for the 100-200 µm SiO_2 spheres in a 1230 µm gap, along with glass wool in the two largest gap sizes of the micro-reactor, where the conversion rises by a factor 1.46, 1.39, and 1.45, respectively. The packing materials seem not to be able to enhance the conversion for gap sizes below 705 µm, which might suggest that the conversion values of the empty reactor are already close to reaching an equilibrium value, and that the back reaction starts to become equally important. Indeed, generating a more powerful plasma will also promote the back reaction more. Furthermore, adding extra material in the reaction zone might introduce more electrical surface losses, which can have a detrimental effect on the overall plasma performance, as seen in the (slightly) lower conversion. The worst result is obtained for the 100-200 µm ZrO_2 spheres in the reactors with gap of 455 and 705 µm, which drastically lower the conversion with 42 %.

It is not possible from these results to distinguish a clear order in the performance of the material type. Either SiO_2, Al_2O_3 or glass wool yield the best results, depending on the bead and gap size combination. ZrO_2 clearly produces the worst results in the smaller size ranges and gaps. It is clear that the size effect is opposite to that observed for the other materials and even (almost) absent for the largest gaps. This suggests that there are a lot of parameters that influence the performance of the materials, besides the dielectric constant, such as the exact material composition, size, shape, surface roughness, electric values, porosity, surface functional groups etc., as also shown by Michielsen et al. [14]. Furthermore, the effect of these parameters can change as well, due to interactions with other factors and with set-up parameters, such as the gap size and SEI. Indeed, a clear difference in 'response' is visible depending on the type of material with changing gap size.

When comparing the micro gap results with the results obtained in the regular sized gap of 4705 µm in Figure 8, the drastic increase in conversion can be seen again, as was also the case for the empty reactor. It is interesting to mention that SiO_2 is typically considered the worst material in the regular gap size [13,14], while it performs as one of the best materials in the micro gap reactor. This is also the case with glass wool, which gave mixed results in other reactors [13,14], while it is clearly one of the best materials in our set-up. Glass wool showed to have no significant improvement in the work of Michielsen et al. [14], compared with the empty reactor, while it does in ours and the work of Duan et al. [13]. This suggests that the performance of glass wool, and perhaps any material, is greatly dependent on the reactor configurations (power, frequency, gap, flow rate, reactor type); and at the right conditions, some materials can become very competitive compared with others, while at other conditions these beneficial aspects might diminish. Glass wool also has the advantages of being more flexible and having a greater specific surface area. Coating glass wool with a catalytic material might be an interesting approach for plasma catalysis, although coating might be experimentally challenging with respect to a reproducible, stable, and uniform coating. In the next sections, the individual effect of the sphere size and gap size will be discussed in more detail.

Influence of sphere size (within same gap size)

For a fixed gap size of 455, 705 or 1230 µm, it can be concluded that for SiO_2 and Al_2O_3 the conversion increases upon reducing the sphere size. The effect is more pronounced for SiO_2 than for Al_2O_3, at least in the 1230 µm gap, where all three sizes were measured. ZrO_2, on the other hand, shows completely the opposite trend, irrespective of the gap size.

These findings might be explained by a few effects occurring at the same time. First of all, smaller spheres will result in more contact points, yielding local field enhancement, and thus will result in a more reactive plasma. This effect was also predicted in modelling work by Van Laer and Bogaerts [34] for a helium plasma in a DBD reactor with 4500 µm gap. The simulations show that indeed the time-averaged electric field strength increases with decreasing sphere size and becomes more spread out

over the whole gap. This should enhance the conversion, as seen with SiO_2 and Al_2O_3. There is, however, a second effect at play in the micro gap reactor. Indeed, other modelling work by Van Laer and Bogaerts [35] shows that in a regular sized reactor the electric field rises by using spheres with a higher dielectric constant. However, it gets more localized between the contact points and the electron density slightly lowers. The same simulations in a micro gap reactor also show a higher electric field, as expected, although more localized at the contact points, and the electron density drastically lowers when the dielectric constant rises from $\varepsilon = 3.9$ (i.e., SiO_2) to $\varepsilon = 25$ (i.e., ZrO_2). This can explain why the impact of Al_2O_3 (ε=9) is slightly less pronounced than that of SiO_2, as well as why ZrO_2 shows the opposite performance, suggesting that the combination of smaller spheres with higher dielectric constant and a micro gap reactor results in a negative outcome in terms of CO_2 conversion. Nevertheless, other, not yet identified material aspects cannot be excluded.

The glass wool fibres might exhibit an analogous behaviour to the 100-200 µm spheres, given the size of the fibres. The number of contact points will be comparable, but the fibrous nature of the glass wool will induce some extra effects. A spherical packing will have at most 12 contact points with neighbouring spheres, while the fibres can have several tens or hundreds of contact points with other fibres. Charge build-up or charge propagation might be diverted and spread out much faster over the neighbouring fibres, resulting in a more homogeneous plasma. It is also possible that the fibres connect the electrode and the dielectric, leading to a short circuit; although this might only be for a short time before polarization of the electrode and the fibre surface opposes the discharge.

Influence of gap size (with same sphere size)

The influence of the gap size was already discussed for the empty reactor (see section 3.1.1), but its effect might be different for the packed reactors, depending on the packing material and sphere size. Figure 8d) shows that the conversion remains about the same upon decreasing gap size when glass wool is put into the micro discharge gaps, compared to the regular sized reactor. This suggests that two phenomena are happening here at the same time. First of all, it looks like glass wool on its own is

a very well performing material, being capable of improving the conversion drastically, even for a relatively large gap size of 1230 μm. However, this improvement will induce the back reaction more as well, so that the reactor reaches an observed maximum CO_2 conversion of around 50 %, defined by the equilibrium with the back reaction, since extra confinement of the gap size to 268 μm does not improve the conversion much further. This behaviour is similar to Figure 7 where a maximum conversion of around 50-55 % was observed, suggesting that the same power driven equilibrium conversion is reached (see section 3.1.3). This is consistent with the high conversion for glass wool, obtained by Duan et al. [13] compared with other packing materials.

Figure 9 presents a combined graph for all sphere materials and sizes, as a function of the gap size. It shows that for most materials the conversion decreases with increasing gap size, which is expected due to the decreasing electric field. The 100-200 μm spheres of SiO_2 and ZrO_2, however, show a somewhat higher conversion in the 1230 μm gap, which cannot yet be explained. In general, the different materials and sphere sizes do not yield very different conversion, with values always between 30 and 50% for all materials, bead sizes and gap sizes, except for the smaller ZrO_2 spheres, which perform somewhat worse. Nevertheless, it is clear from this figure that depending on the gap size, other materials should be chosen to reach the highest conversion.

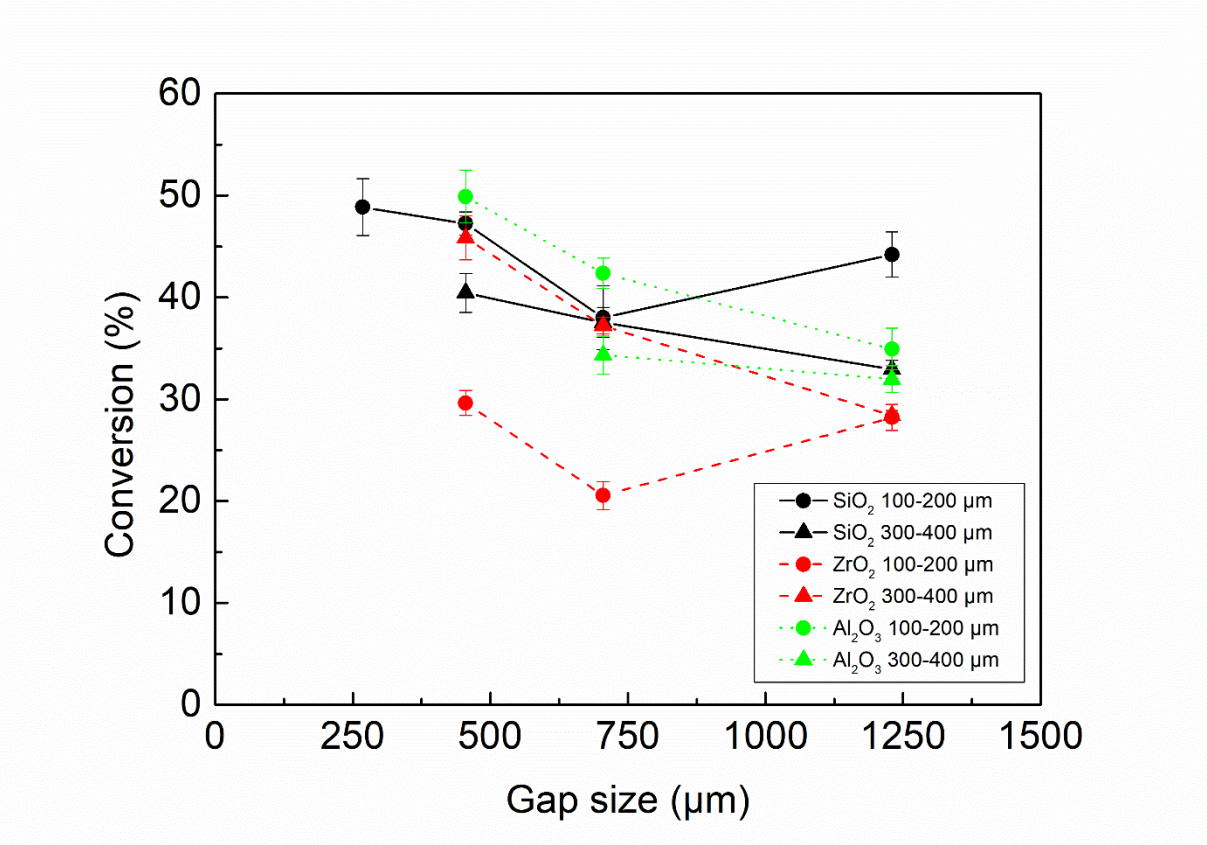

Figure 9: Conversion for different materials and sphere sizes, as a function of gap size, throughout the micro gap size range, at a constant residence time of 7.5 s and 30 W plasma power.

3.2.2 Electrical characterization

In an attempt to reveal the underlying mechanisms of the improvements in conversion observed in 3.2.1, electrical characterization was performed as well for the packed reactors. Figure 10 illustrates as an example the Lissajous plots for the packed bed reactor with 1230 μm gap, packed with the 300-400 μm spheres of different materials, as well as glass wool. Electrical differences are noticeable between the different materials for the maximum voltage, maximum charge, and burning voltage, but also subtle changes can be observed in the effective capacitance ζ_{diel} and the resulting partial discharging α (see details in the SI). It is also visible that a packing material can influence the discharge and capacitive phase. For example, zirconia and alumina show a relatively short capacitive phase and a long discharge phase, while silica and glass wool show a relatively long capacitive phase and a shorter discharge phase.

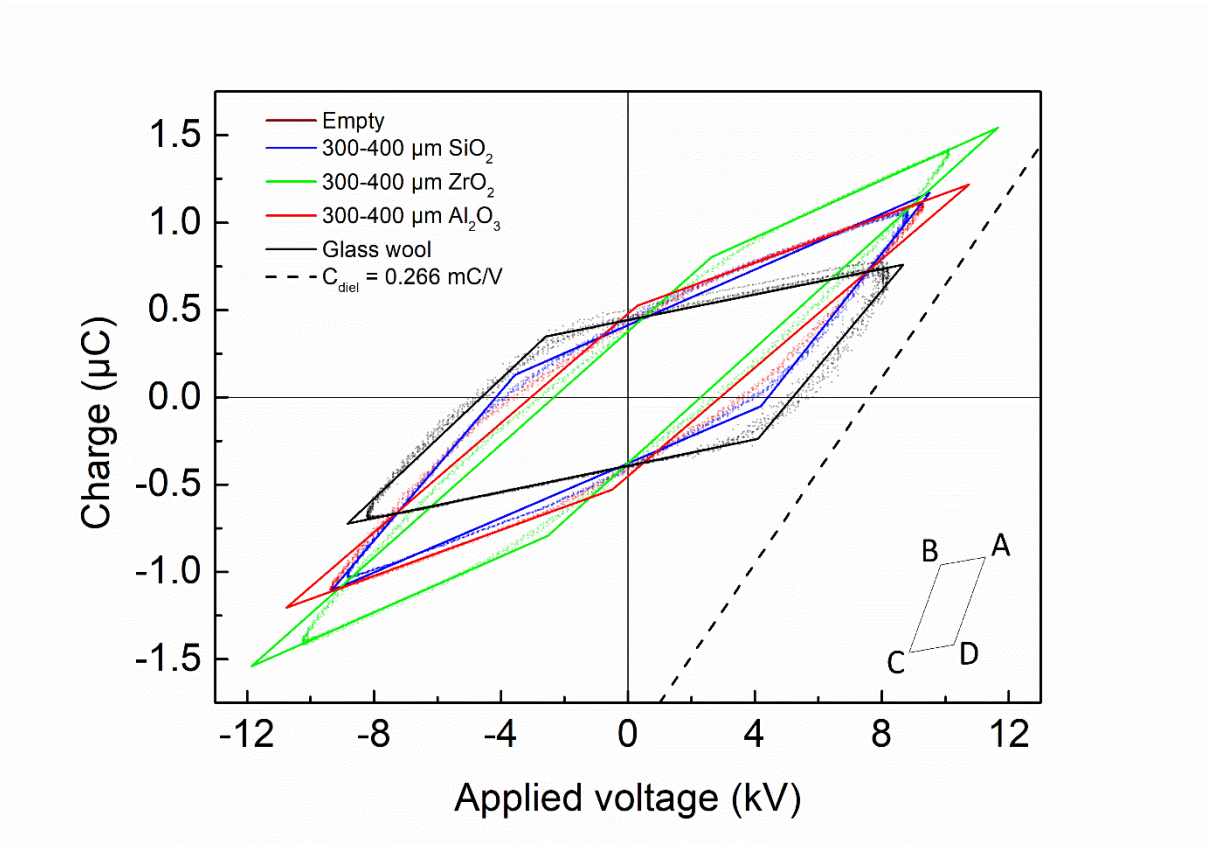

Figure 10: Raw Lissajous plots (dotted) for a DBD micro reactor with a gap size of 1230 µm packed with different packing materials (see legend) for a constant residence time of 7.5 s, as well as the slopes calculated by the MATLAB script (solid lines). Comparison is also made with the C_{diel} value of a completely discharged reactor (dashed line).

These characteristics change even more with varying sphere and gap size. The investigated parameters in this electrical characterization are again the peak-to-peak voltage (U_{pp}), root-mean-square current (I_{RMS}), effective capacitance (ζ_{diel}), partial discharging fraction (α), burning voltage (U_{bur}), number of micro discharges per period, and displaced charge per micro discharge, as in section 3.1.2. A lot of data is retrieved this way with multiple parameters changed between them, being the material type, material size and gap size. Besides the effect of the packing materials, which can influence the electrical characteristics of the plasma; these electrical parameters can influence the packing material behaviour as well, resulting in coupled interactions until a steady-state like behaviour is reached. In addition, all the possible inter-electrical and inter-material interactions should be considered. There might be more parameters that have to be taken into account to fully understand the electrical, physical, and chemical behaviour of the plasma in packed bed reactors; therefore, it is still very complicated to draw

fundamental conclusions. This makes it particularly difficult to pinpoint the underlying mechanisms of the conversion results presented in section 3.2.1, although a number of observations can be made.

The detailed trends of the electrical characteristics for the various materials, bead sizes and gap sizes are plotted in the SI (see Figures S2-S8). In general, it can be seen that most of the electrical parameters still follow the same trends as seen in the empty reactor (section 3.1.2). They do, however, differ between the different packing materials and sizes. Significant trends can be seen for the peak-to-peak voltage, RMS current and the partial discharging behaviour of the plasma for the different sphere sizes. These trends are, however, very dependent on the specific material being used. Some are even completely opposite, suggesting that there are multiple effects at play, influencing the resulting conversion. The burning voltage, on the other hand, is completely unaffected by material composition and sphere size and thus only controlled by the gap size. The number of current pulses is a lot higher, but the pulses are weaker, compared to the empty reactor. Up to 512 micro discharges were observed in the packed reactor, with a maximum transferred charge of 5.9 nC/discharge, while the empty reactor had only a maximum of 49 micro discharges, but with a maximum of 59 nC/discharge.

3.2.3 Efficiency

In Figure 8 we showed that adding a packing material to the reactor can indeed drastically enhance the conversion by a factor 3.47, when compared to an empty reactor with the same residence time, and some materials yield even better conversion than the empty reactor with the same flow rate but a residence time almost four times as long. In Figure 11 the results of the energy efficiency are plotted to check if the packed bed micro gap reactors can do better overall. Only the energy efficiency is plotted here, since dissociation rate and energy yield show exactly the same trend at a constant power input, with only a difference of a constant factor, i.e. 0.065 mmol/min% and 0.130 mmol/Wh%, respectively.

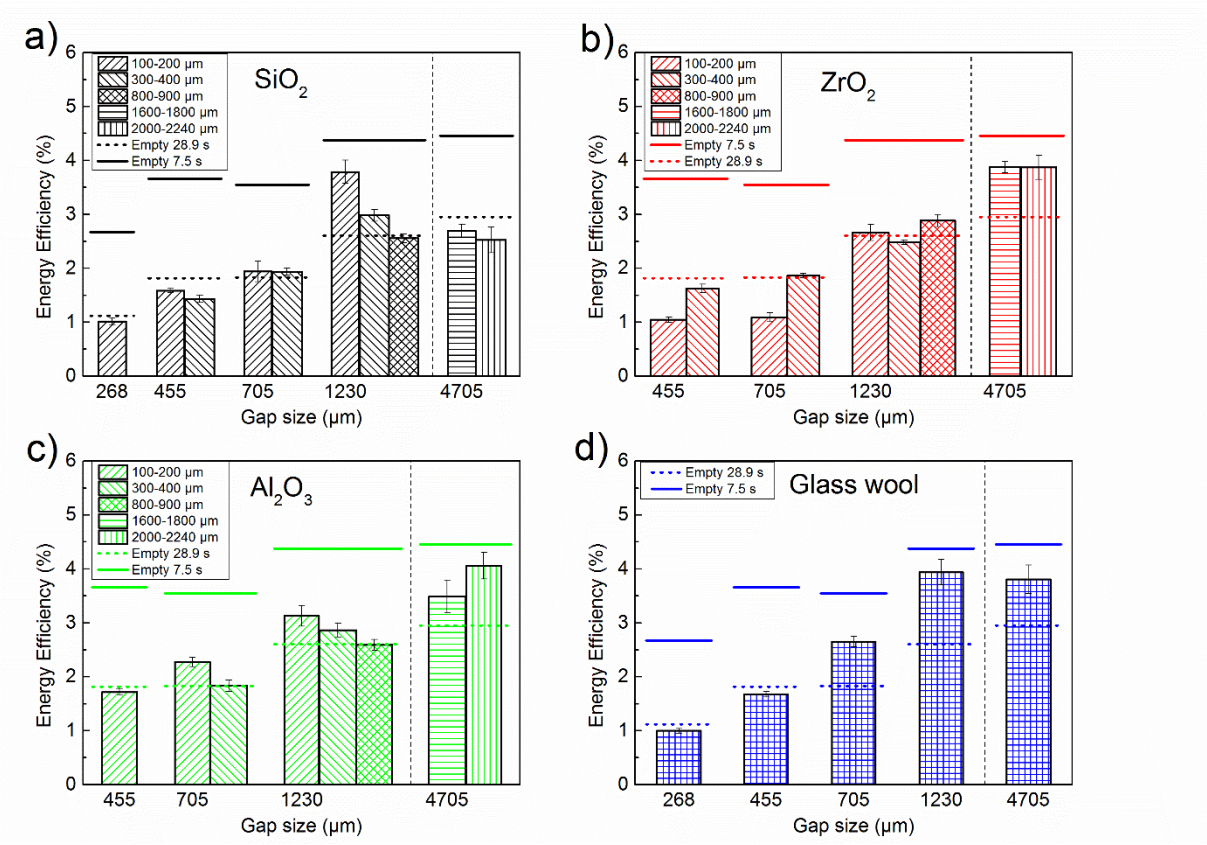

Figure 11: Energy efficiency in packed bed DBD (micro) reactors for a constant residence time of 7.5 s and plasma power of 30 W. The results are displayed per material type for different sphere sizes (indicated by the legend) and as a function of gap size, and compared to the empty reactor at the same residence time of 7.5 s (solid horizontal lines) and a residence time of 28.9 s (corresponding to the same flow rate as the packed bed reactors) (dashed horizontal lines).

The 'material-size-gap' combinations that showed a better conversion than the empty micro gap reactor with 28.9 s residence time (hence same flow rate as the packed bed reactor) also show better energy efficiencies (cf. the small horizontal dashed lines), which is logical since the energy efficiency is proportional to the conversion and all the other parameters in the formula (i.e., power, flow rate; see eq. (3)) are the same. Thus, adding a packing material to the reactor, while maintaining the same throughput, increases the efficiency slightly, depending on the material type and size. The best results are obtained in the 1230 µm gap, filled with either 100-200 µm SiO_2 spheres or glass wool; or the original 4705 µm gap with ZrO_2, Al_2O_3, or glass wool packing. In general, glass wool performs best, followed by Al_2O_3, as it yields an improvement in the 705 µm gap, as well as in the regular sized reactor.

On the other hand, while the conversions improved significantly when compared to the empty reactor at the same residence time of 7.5 s (see Figure 8 above), this improvement is not reflected in the

efficiency results, when compared with the empty reactor at the same contact time of 7.5 s. Indeed, the almost four times decrease in flow rate (which negatively affects the energy efficiency, cf. eq. (3)) is not compensated by a sufficient increase in conversion (which was typically around a factor of 2). The 'material-size-gap' combinations that come closest to the empty reactor at the same residence time are again the 1230 µm gap, filled with either 100-200 µm SiO_2 spheres or glass wool, i.e., the same as above. These materials perform remarkably well, certainly keeping in mind their low dielectric constant, and because the conversion is rather low in the empty reactor at this relatively large gap size, they seem to have more room to improve, before they reach the observed maximum conversion of around 50-55 %, dictated by the equilibrium with the back reaction, see section 3.1.3.

It can also be deduced from the energy efficiency data that the larger gap size reactors without any packing material show the highest energy efficiency. It should, however, be noted that the performance of the packed bed reactors was not tested at the flow rates corresponding to those of the empty reactor at 7.5 s residence time. This will result in an even shorter residence time of only 1.9 s, yielding a lower conversion. For some 'material-size-gap' combinations, the conversion will probably still be higher than in the empty reactor (as can be deduced from Figure 8), and therefore in the end perhaps still slightly higher efficiencies could be expected (probably around 5-5.5 %, if the same trends can be expected as for the larger residence time).

Finally, it can be concluded from all our results that the best performing 'material-size-gap' combination, in terms of both conversion and energy efficiency, at the conditions investigated here (reactor type, reactor shape, power and frequency) corresponds to a gap size between 1230 and 4705 µm, with smaller sized spheres (mainly of SiO_2 or Al_2O_3), or glass wool as packing material, at elevated flow rates.

4 Conclusion

In this study, we investigated the effect of gap size, as well as packing material and sphere size, on the CO_2 conversion and corresponding energy efficiency, in both empty and packed bed DBD reactors. We

focused especially on micro gap size reactors (268-1230 μm), but also made the comparison with a regular sized reactor of 4705 μm. Reducing the gap size was shown to significantly enhance the conversion, compared to a regular size DBD reactor, both in an empty reactor and packed bed reactor. In the empty reactor, the conversion could rise up to 33 % and 54 % at a residence time of 7.5 s and 28.9 s, respectively, in the smallest gap size. The effect of residence time was further investigated in a gap size of 455 μm and revealed an increasing conversion up to 30 s before levelling off to a maximum conversion of around 50-55 %. At the same time, thorough analysis of the Lissajous figures showed that reducing the gap size provides a more uniformly ignited reactor, with a larger amount of micro-discharges and a larger displaced charge in the discharge phase of the reactor, which can explain the higher conversion. This might be related to the higher reduced electric field and power density (resulting from the same applied voltage/power over a smaller gap/volume).

The influence of adding a packing material was greatly dependent on the type of material being used, the corresponding size and the discharge gap. In contrast to results obtained in a regular sized reactor [13,14], silica and glass wool gave the best improvements in conversion, next to alumina, with maximum conversions reaching around 50 %. Furthermore, the effect of size of the packing material is greatly dictated by the material being used. Silica and alumina show better results with decreasing sphere size for a given gap size, while zirconia shows the opposite trend. Electrical analysis of the Lissajous figures showed that several known and unknown parameters might play a role in determining the conversion. The effect of partial discharging, burning voltage, number of micro-discharges, displaced charge, peak-to-peak voltage and current was discussed, and we can conclude that a lot of parameters might play a role in determining the obtained conversion results. Systematic synthesizing and testing of packing materials in a controlled environment, such as the apparatus proposed by Butterworth and Allen [36] with one or multiple spheres, might be needed here to pinpoint the exact role of each of these parameters.

While the conversion significantly increased upon decreasing gap size and upon adding a packing in the reactor, the corresponding efficiency shows less impressive results. For the empty reactor, the regular gap size (4705 µm) appears to be the most energy efficient configuration, despite the immense increase in conversion obtained upon gap size reduction. The maximum energy efficiency obtained was 4.3 %. In general, the efficiency was found to be better in the larger gap sizes, when comparing at the same residence time, which is logical as larger gap sizes yield a (significantly) higher flow rate for the same residence time, and the energy efficiency is proportional to both conversion and flow rate. When the reactor was packed with different materials, some 'material-size-gap' combinations yielded higher efficiency compared with the same flow rate in the empty reactor, but when compared at the same residence time, the energy efficiency was always lower than in the empty reactor.

So now we are able to answer the question: Does size matter? The answer is definitely yes. However, the next question is: How does it matter? As illustrated in this paper, the answer will depend on which specific size, i.e., of the gap or spheres, which type of the material and which desired effect is aimed at, i.e., increased conversion and/or efficiency. We have to be careful when studying the effect of packing materials in DBD reactors. It is almost impossible to predict their exact behaviour, since there are numerous unknown variables of the materials, as well as intertwined parameters of the material-reactor configuration, such as dielectric constant and gap size. This stresses the need for systematic experiments of different material-reactor combinations. The conclusions drawn in this paper therefore apply to pure CO_2 splitting, and cannot necessarily be generalized to other systems. To draw conclusions for other gases or mixtures, dedicated experiments should be performed. With this work, we contributed to gain some insight in these complex and intertwined effects.

Acknowledgements

We acknowledge financial support from the European Fund for Regional Development through the cross-border collaborative Interreg V program Flanders-the Netherlands (project EnOp), the Fund for

Scientific Research (FWO; grant number: G.0254.14N) and an IOF-SBO (SynCO2Chem) project from the University of Antwerp.

References

[1] H.-H. Kim, Nonthermal Plasma Processing for Air-Pollution Control: A Historical Review, Current Issues, and Future Prospects, Plasma Process. Polym. 1 (2004) 91–110. doi:10.1002/ppap.200400028.

[2] J. Van Durme, J. Dewulf, C. Leys, H. Van Langenhove, Combining non-thermal plasma with heterogeneous catalysis in waste gas treatment: A review, Appl. Catal. B Environ. 78 (2008) 324–333. doi:10.1016/j.apcatb.2007.09.035.

[3] U. Kogelschatz, B. Eliasson, W. Egli, From ozone generators to flat television screens: history and future potential of dielectric-barrier discharges, Pure Appl. Chem. 71 (1999) 1819–1828. doi:10.1351/pac199971101819.

[4] U. Kogelschatz, Dielectric-barrier Discharges: Their History, Discharge Physics, and Industrial Applications, 23 (2003) 1–46.

[5] R. Snoeckx, A. Bogaerts, Plasma technology – a novel solution for CO_2 conversion?, Chem. Soc. Rev. 46 (2017) 5805–5863. doi:10.1039/C6CS00066E.

[6] A. Bogaerts, E. Neyts, R. Gijbels, J. van der Mullen, Gas discharge plasmas and their applications, Spectrochim. Acta - Part B At. Spectrosc. 57 (2002) 609–658. doi:10.1016/j.sab.2004.03.009.

[7] A.M. Vandenbroucke, R. Morent, N. De Geyter, C. Leys, Non-thermal plasmas for non-catalytic and catalytic VOC abatement, J. Hazard. Mater. 195 (2011) 30–54. doi:10.1016/j.jhazmat.2011.08.060.

[8] X. Tu, J.C. Whitehead, Plasma-catalytic dry reforming of methane in an atmospheric dielectric barrier discharge: Understanding the synergistic effect at low temperature, Appl. Catal. B Environ. 125 (2012) 439–448. doi:10.1016/j.apcatb.2012.06.006.

[9] K. Van Laer, A. Bogaerts, Fluid modelling of a packed bed dielectric barrier discharge plasma reactor, Plasma Sources Sci. Technol. 25 (2016) 15002. doi:10.1088/0963-0252/25/1/015002.

[10] Y.R. Zhang, K. Van Laer, E.C. Neyts, A. Bogaerts, Can plasma be formed in catalyst pores? A modeling investigation, Appl. Catal. B Environ. 185 (2016) 56–67. doi:10.1016/j.apcatb.2015.12.009.

[11] E.C. Neyts, A. Bogaerts, Understanding plasma catalysis through modelling and simulation—a review, J. Phys. D. Appl. Phys. 47 (2014) 224010. doi:10.1088/0022-3727/47/22/224010.

[12] E.C. Neyts, K. Ostrikov, M.K. Sunkara, A. Bogaerts, Plasma Catalysis: Synergistic Effects at the Nanoscale, Chem. Rev. 115 (2015) 13408–13446. doi:10.1021/acs.chemrev.5b00362.

[13] X. Duan, Z. Hu, Y. Li, B. Wang, Effect of dielectric packing materials on the decomposition of carbon dioxide using DBD microplasma reactor, AIChE J. 61 (2015) 898–903. doi:10.1002/aic.

[14] I. Michielsen, Y. Uytdenhouwen, J. Pype, B. Michielsen, J. Mertens, F. Reniers, V. Meynen, A. Bogaerts, CO_2 dissociation in a packed bed DBD reactor: First steps towards a better understanding of plasma catalysis, Chem. Eng. J. 326 (2017) 477–488. doi:10.1016/j.cej.2017.05.177.

[15] T. Butterworth, R. Elder, R. Allen, Effects of particle size on CO_2 reduction and discharge

characteristics in a packed bed plasma reactor, Chem. Eng. J. 293 (2016) 55–67. doi:10.1016/j.cej.2016.02.047.

[16] S. Kameshima, K. Tamura, Y. Ishibashi, T. Nozaki, Pulsed dry methane reforming in plasma-enhanced catalytic reaction, Catal. Today. 256 (2015) 67–75. doi:10.1016/j.cattod.2015.05.011.

[17] D. Mei, X. Zhu, Y. He, J.D. Yan, X. Tu, Plasma-assisted conversion of CO_2 in a dielectric barrier discharge reactor : understanding the effect of packing materials, Plasma Sources Sci. Technol. 24 (2015) 15011. doi:10.1088/0963-0252/24/1/015011.

[18] M. Kraus, B. Eliasson, U. Kogelschatz, A. Wokaun, CO2 reforming of methane by the combination of dielectric-barrier discharges and catalysis, Phys. Chem. Chem. Phys. 3 (2001) 294–300.

[19] Y.F. Guo, D.Q. Ye, K.F. Chen, J.C. He, Toluene removal by a DBD-type plasma combined with metal oxides catalysts supported by nickel foam, Catal. Today. 126 (2007) 328–337. doi:10.1016/j.cattod.2007.06.025.

[20] J.C. Whitehead, Plasma – catalysis : the known knowns , the known unknowns and the unknown unknowns, J. Phys. D. Appl. Phys. 49 (2016) 243001. doi:10.1088/0022-3727/49/24/243001.

[21] U. Kogelschatz, Applications of microplasmas and microreactor technology, Contrib. to Plasma Phys. 47 (2007) 80–88. doi:10.1002/ctpp.200710012.

[22] A. Aĝiral, T. Nozaki, M. Nakase, S. Yuzawa, K. Okazaki, J.G.E. Han Gardeniers, Gas-to-liquids process using multi-phase flow, non-thermal plasma microreactor, Chem. Eng. J. 167 (2011) 560–566. doi:10.1016/j.cej.2010.10.050.

[23] M. Bai, Z. Zhang, M. Bai, X. Bai, H. Gao, Synthesis of Ammonia using CH_4/N_2 plasmas based on micro-gap discharge under environmentally friendly condition, Plasma Chem. Plasma Process. 28 (2008) 405–414. doi:10.1007/s11090-008-9132-4.

[24] H. Sekiguchi, M. Ando, H. Kojima, Study of hydroxylation of benzene and toluene using a micro-DBD plasma reactor, J. Phys. D. Appl. Phys. 38 (2005) 1722–1727. doi:10.1088/0022-3727/38/11/013.

[25] J. Pype, B. Michielsen, E.M. Seftel, S. Mullens, V. Meynen, Development of alumina microspheres with controlled size and shape by vibrational droplet coagulation, J. Eur. Ceram. Soc. 37 (2017) 189–198. doi:10.1016/j.jeurceramsoc.2016.07.020.

[26] S. Paulussen, B. Verheyde, X. Tu, C. De Bie, T. Martens, D. Petrovic, A. Bogaerts, B. Sels, Conversion of carbon dioxide to value-added chemicals in atmospheric pressure dielectric barrier discharges, Plasma Sources Sci. Technol. 19 (2010) 34015. doi:10.1088/0963-0252/19/3/034015.

[27] A. Ozkan, A. Bogaerts, F. Reniers, Routes to increase the conversion and the energy efficiency in the splitting of CO_2 by a dielectric barrier discharge, J. Phys. D. Appl. Phys. 50 (2017) 84004. doi:10.1088/1361-6463/aa562c.

[28] O. Levenspiel, Chemical Reaction Engineering Third Edition, 1999. doi:10.1021/ie990488g.

[29] N. Pinhão, A. Moura, J.B. Branco, J. Neves, Influence of gas expansion on process parameters in non-thermal plasma plug-flow reactors: A study applied to dry reforming of methane, Int. J. Hydrogen Energy. 41 (2016) 9245–9255. doi:10.1016/j.ijhydene.2016.04.148.

[30] R. Snoeckx, S. Heijkers, K. Van Wesenbeeck, S. Lenaerts, A. Bogaerts, CO_2 conversion in a dielectric barrier discharge plasma: N_2 in the mix as a helping hand or problematic impurity?, Energy Environ. Sci. Energy Environ. Sci. 9 (2016) 999–1011. doi:10.1039/c5ee03304g.

[31] T.C. Manley, The electric characteristics of the ozonator discharge, Trans. Electrochem. Soc. 84 (1943) 83–96.

[32] R. Aerts, W. Somers, A. Bogaerts, Carbon Dioxide Splitting in a Dielectric Barrier Discharge Plasma: A Combined Experimental and Computational Study, ChemSusChem. 8 (2015) 702–716. doi:10.1002/cssc.201402818.

[33] B. Wang, W. Yan, W. Ge, X. Duan, Kinetic model of the methane conversion into higher hydrocarbons with dielectric barrier discharge micro-plasma reactor, Chem. Eng. J. 234 (2013) 354–360. doi:10.1016/S2095-4956(14)60267-9.

[34] K. Van Laer, A. Bogaerts, How bead size and dielectric constant affect the plasma behaviour in a packed bed plasma reactor: A modelling study, Plasma Sources Sci. Technol. 26 (2017). doi:10.1088/1361-6595/aa7c59.

[35] K. Van Laer, A. Bogaerts, Influence of Gap Size and Dielectric Constant of the Packing Material on the Plasma Behaviour in a Packed Bed DBD Reactor: A Fluid Modelling Study, Plasma Process. Polym. 14 (2017). doi:10.1002/ppap.201600129.

[36] T. Butterworth, R.W.K. Allen, Plasma-catalyst interaction studied in a single pellet DBD reactor: Dielectric constant effect on plasma dynamics, Plasma Sources Sci. Technol. 26 (2017). doi:10.1088/1361-6595/aa6c35.

A packed-bed DBD micro plasma reactor for CO_2 dissociation: Does size matter?
Supplementary information

Y. Uytdenhouwen [a,b], S. Van Alphen [a], I. Michielsen [a,b], V. Meynen [b], P. Cool [b], A. Bogaerts [a]

[a] Research Group PLASMANT, Department of Chemistry, University of Antwerp, Universiteitsplein 1, Wilrijk B-2610, Belgium

[b] Research Group LADCA, Department of Chemistry, University of Antwerp, Universiteitsplein 1, Wilrijk B-2610, Belgium

1 Electrical characterization: Theory

Figure 2 of the main paper shows a typical oscillogram and a simplified Lissajous figure. The oscillogram obtained from each experiment can be directly analysed to calculate the peak-to-peak voltage (U_{pp}) and root-mean-square current (I_{RMS}) of the plasma reactor.

Further analysis of the Lissajous figures gives information about the electrical behaviour of the plasma. The Lissajous figure can be divided into four regions, representing the four phases occurring during one voltage period. They consist of two capacitive phases, AB and CD, where the reactor behaves like a capacitor with no activity in the reaction volume; as well as two discharge phases, BC and DA, where the gas present in the reaction volume is (partially) transformed into a plasma and a net flow of electrons through the reactor is present, resulting in a combined resistive-capacitive behaviour of the reactor. The Q-U Lissajous figure has the benefit that the slopes directly relate to a physical value, i.e. the capacitance of the reactor during that specific phase, since $dQ/dU = C$. In the capacitive phases, the slopes show the total capacitance of the reactor C_{cell} which can be represented in a simplified electrical model, shown in Figure S1a), by two capacitors in series, representing the capacitance of the dielectric barrier C_{diel} and the discharge gap C_{gap} according to the following equation:

$$\frac{1}{C_{cell}} = \frac{1}{C_{diel}} + \frac{1}{C_{gap}} \qquad \text{(SI1)}$$

In the discharge phase, the charge built up by the applied voltage reaches a threshold, which ignites the plasma. The capacitance of the discharge gap is then electrically bypassed due to the conductivity of the plasma and only the capacitance of the dielectric barrier remains, shown by the respective slopes. This phase is depicted in the simplified model by the dielectric barrier capacitance bypassed by a low value resistor. In the capacitance phase the model uses an infinitely high value resistor.

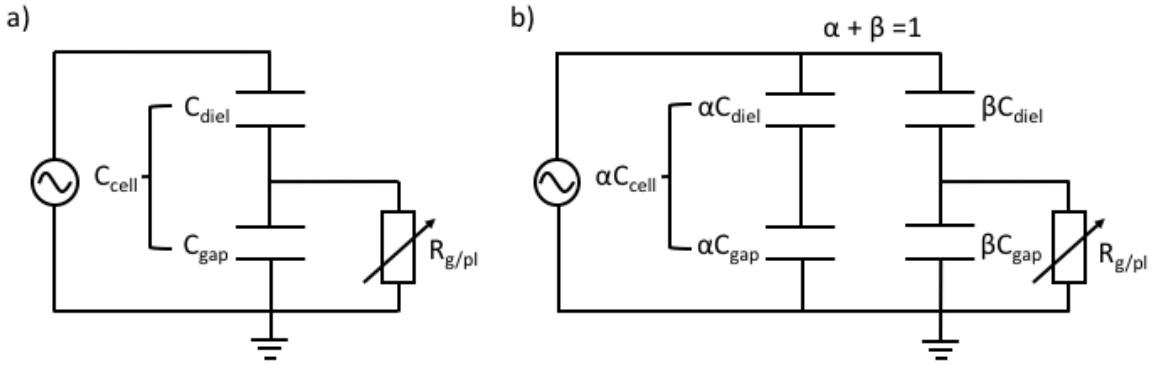

Figure S1: a) Simplified electrical model for a DBD reactor. b) Extended model for a DBD reactor incorporating partial discharging.

The flaw with this model is its assumption of a fully discharged reaction volume, leaving only the capacitance of the dielectric tube C_{diel} as the source of the slope of the discharge phase. However, if the reaction volume is not entirely discharged and not all accumulated charge is used, we get an intermediate phase, i.e., a partial discharge, with an effective capacitance and slope ζ_{diel} that has a value between C_{diel} and C_{cell}, depending on the degree of partial discharging. A new model was proposed by Peeters and van de Sanden [1] to accommodate this partial discharging of the DBD reactor, as shown in Figure S1b). The electrical model is now divided into two parts: a non-discharging α part and a discharging β part. When the reactor is in the discharge phase, the volume α of the reactor that is not ignited is now represented by a partial capacitance for the dielectric barrier and the discharge gap; while the ignited volume β is represented by the complementary capacitances configured like the original model. However, during the capacitive phase of the reactor, the resistor in the β part again has an infinitely high value, resulting in the cumulated capacitive behaviour of the dielectric barrier and reaction volume like before. Using this model, the fraction of partial discharging can now be quantified and used as a measure of efficient behaviour of a particular reactor setup. This fraction of partial discharging α is calculated by the formula of Peeters and van de Sanden [1]:

$$\alpha = \frac{C_{diel} - \zeta_{diel}}{C_{diel} - C_{cell}} \qquad \text{(SI2)}$$

C_{cell} and ζ_{diel} can directly be determined by calculating the respective slopes of the Lissajous figure; the capacitance of the ideal, fully discharged reactor C_{diel} however, cannot. Butterworth et al. [2] showed that this value can be obtained by using an argon plasma, making this the closest approximation compared with roughly calculated values, since this method uses the actual reactor set-up. A dielectric capacitance C_{diel} of 26.6 ± 0.2 mC/V is measured, independent of the discharge gap size.

Next, the burning voltage can be determined. The burning voltage is the minimum voltage required to maintain the plasma discharge during the experiment and is normally determined in the Lissajous figure as half of the voltage difference between the intersects with the x-axis. This value needs to be corrected for the partial discharging of the reactor according to the formula of Peeters and van de Sanden [1]:

$$U_{\mathrm{bur}} = \frac{1 - C_{cell}/C_{diel}}{1 - C_{cell}/\zeta_{diel}} \Delta U \qquad \text{(SI3)}$$

Finally, the displaced charge during the discharge phase Q_{disp} and the number of micro discharges are calculated. This is done to analyse the average strength of the discharges. The displaced charge Q_{disp} is calculated by taking the difference in charge between points A and D in the Lissajous figure, see also figure 2 in the main paper. Individual micro discharges are determined after normalization of the current profile and applying height and width threshold values to exclude signal noise, resonance, and systematic measuring errors. The Picoscope 6402D oscilloscope from Picotech used a sample rate of 625 MS/s in our set-up, corresponding to a sample interval of 1.6 ns, which is well below the typical duration of a micro discharge of around (a few) hundred nano seconds. Different threshold values were used for empty and packed reactors due to the large difference in discharge intensity (width and height). This does mean that not every single discharge in the reactor can be measured, e.g. if they are too short, too small, or coincide with a bigger peak or resonance. Therefore, the returned value will not be the exact number of discharges in the plasma but will still be a systematically calculated and representable number.

2 Electrical characterization: Results of the packed reactor

To explain the results of conversion in the packed reactor for different gap-sphere-material combinations, we can again look at the electrical characteristics, like in the empty reactor, although the underlying mechanisms are more complicated than in the empty reactor, due to many intertwined effects.

For the peak-to-peak voltage, three general trends are visible in Figure S2. First, smaller gaps require somewhat lower voltages to maintain a constant plasma power of 30 W for a constant sphere size, which was not the case in the empty reactor, as shown in section 3.1.2 of the main paper. Second, smaller spheres in a certain gap size require a larger voltage to maintain the plasma power. Although the local inter-sphere discharge gap is smaller and should ignite quicker, the larger number of spheres require a greater applied potential to be distributed over each sphere-gap-sphere micro reactor. Third, the general order of materials requiring an increasing voltage is glass wool < silica < alumina < zirconia.

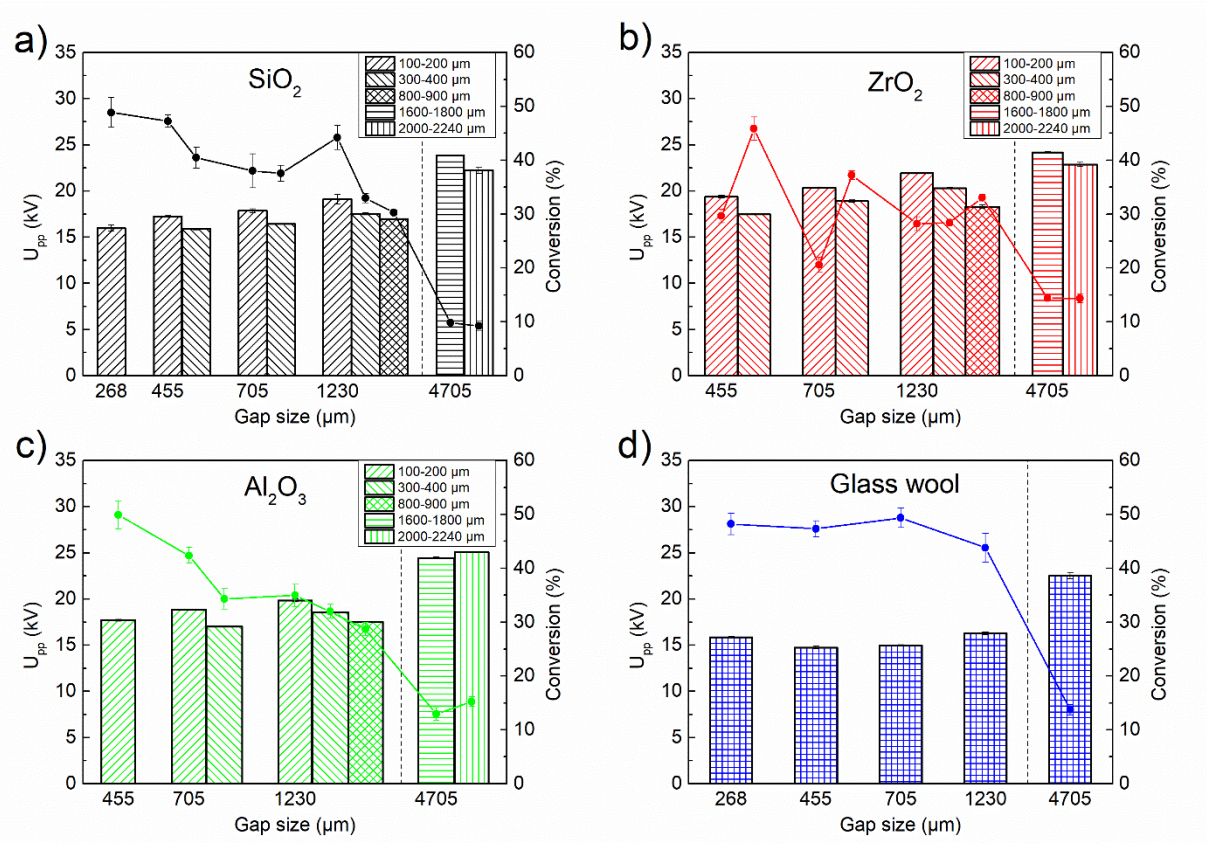

Figure S2: Peak-to-peak voltage of packed bed DBD (micro) reactors at a constant residence time of 7.5 s. Results are displayed per material type for different sphere sizes (as indicated by the legend) and as a function of gap size, and compared to the conversion of the corresponding packed reactor (solid line).

The RMS current shows partially the same trends in Figure S3. The current flowing through the reactor is slightly higher with smaller spheres and the same overall order of materials as with the peak-to-peak voltage is found. It does raise the question why zirconia needs the highest voltage and current, while the conversion is lower than the other materials. A suggestion might be that zirconia has a more electrically conductive behaviour than the other materials and that more of the applied power is lost due to surface losses.

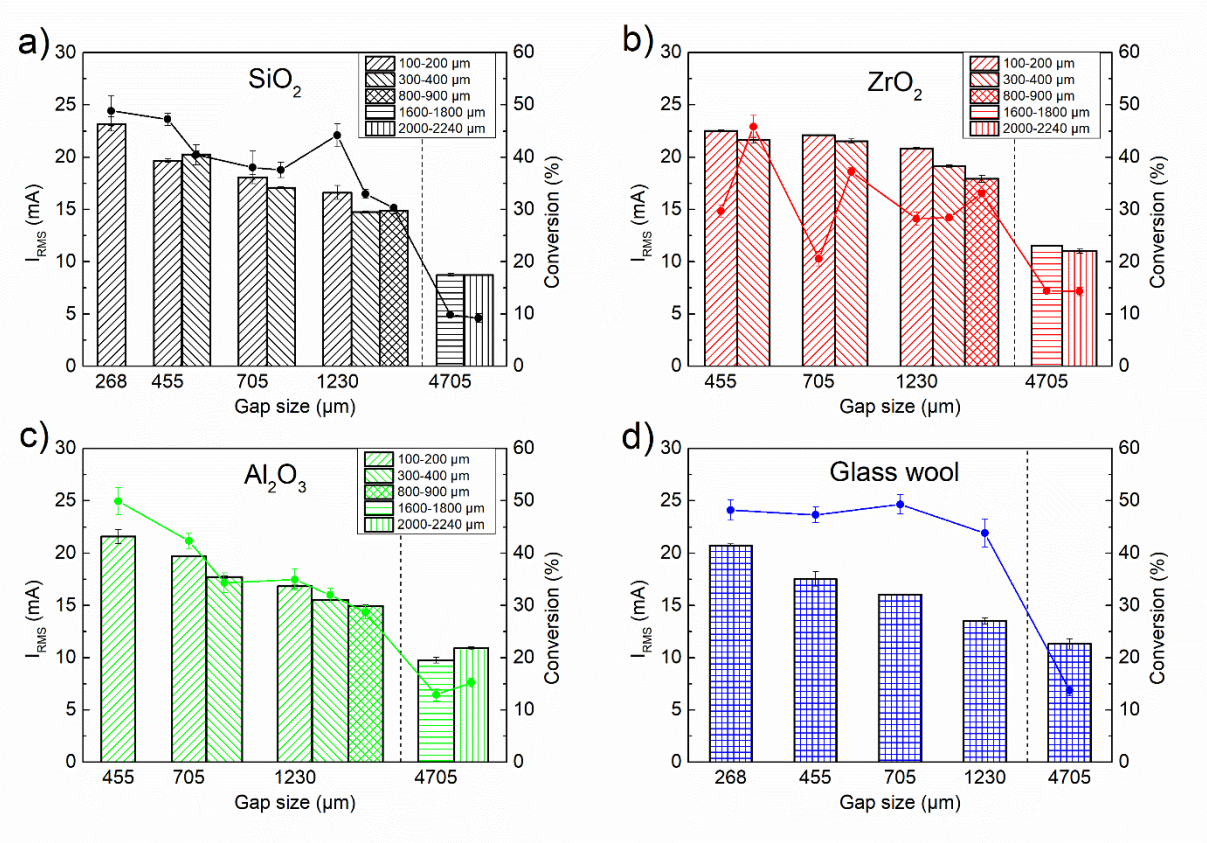

Figure S3: Average current flow (root mean square) of packed bed DBD (micro) reactors at a constant residence time of 7.5 s. Results are displayed per material type for different sphere sizes (as indicated by the legend) and as a function of gap size, and compared to the conversion of the corresponding packed reactor (solid line).

The effective capacitance and the derived partial discharging fraction of the reactor, displayed in Figure S4 and Figure S5, show some counterintuitive trends. The trend of the empty reactor, where a smaller discharge gap results in less partial discharging and thus a higher conversion, is still visible. However, this is clearly material dependent, as the decrease of α follows the order glass wool >> silica > alumina / zirconia Moreover, in packed bed reactors, less partial discharging does not always mean higher conversion. Zirconia spheres within a fixed discharge gap cohere to this trend, but silica and alumina show the opposite results. It shows that decreasing the sphere size leads to more partial discharging, since the plasma cannot be so easily ignited, but that the conversion still increases. Glass wool shows very low partial discharging behaviour with some of the highest conversions as a result.

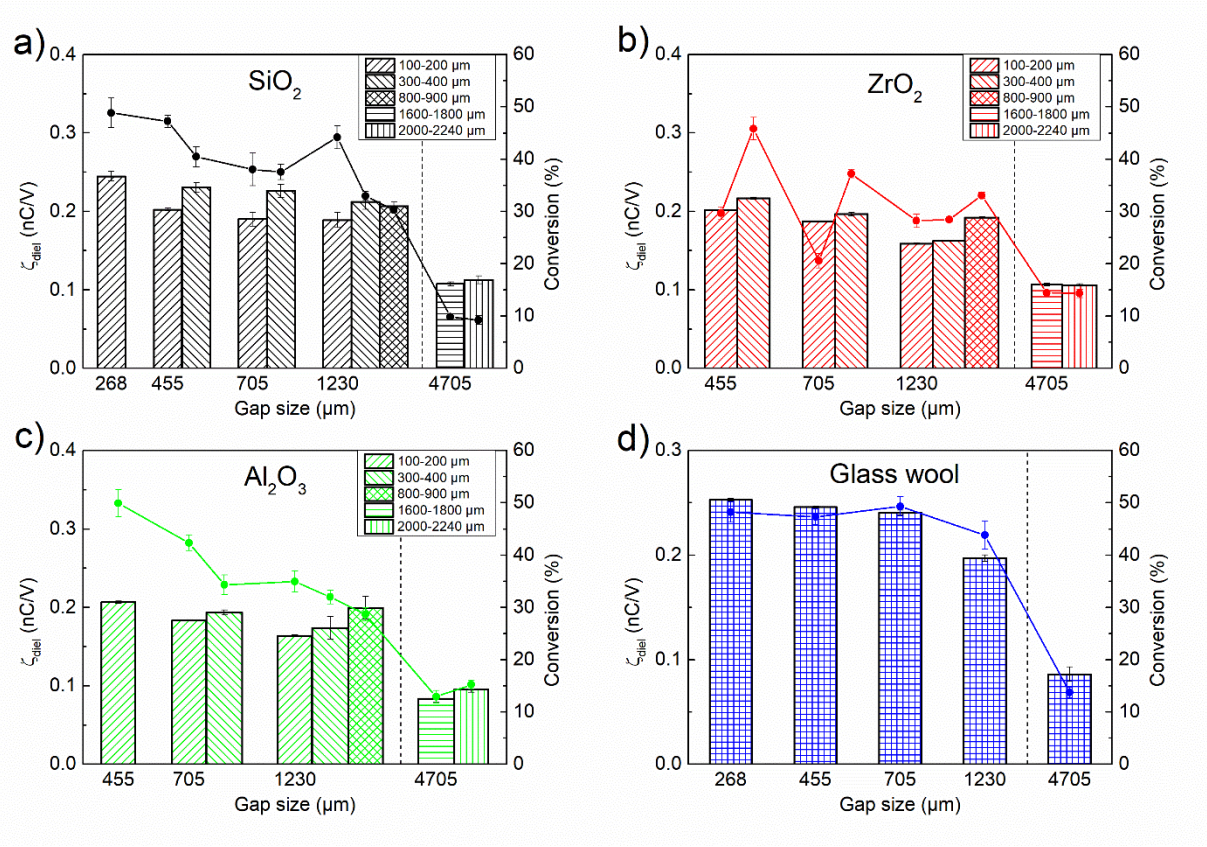

Figure S4: Effective capacitance of packed bed DBD (micro) reactors at a constant residence time of 7.5 s. Results are displayed per material type for different sphere sizes (as indicated by the legend) and as a function of gap size, and compared to the conversion of the corresponding packed reactor (solid line).

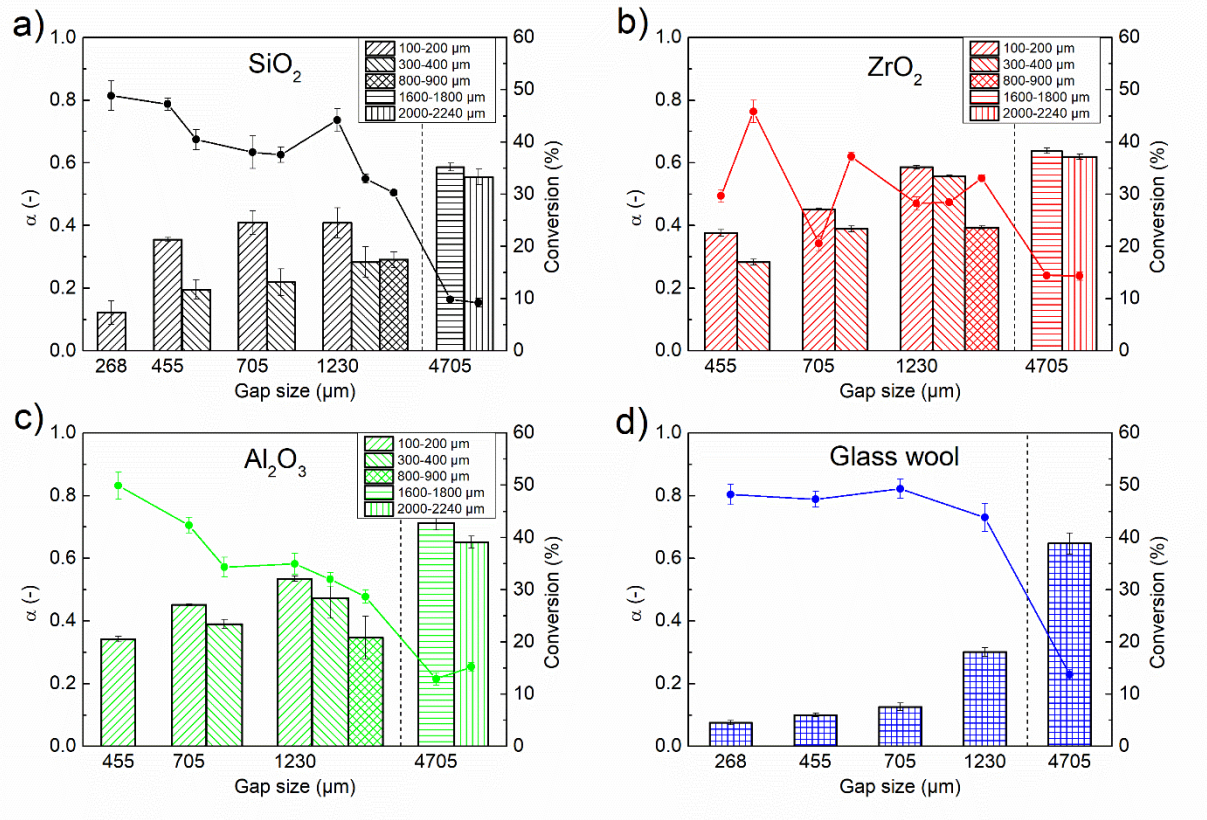

Figure S5: Partial discharging of packed bed DBD (micro) reactors at a constant residence time of 7.5 s. Results are displayed per material type for different sphere sizes (as indicated by the legend) and as a function of gap size, and compared to the conversion of the corresponding packed reactor (solid line).

The burning voltage does not reveal any clear trends, as seen in Figure S6, aside from being mostly discharge gap dependent. Silica, alumina and glass wool give comparable results, while zirconia is the only exception. It requires the lowest burning voltage, but in contrast the highest peak-to-peak voltage.

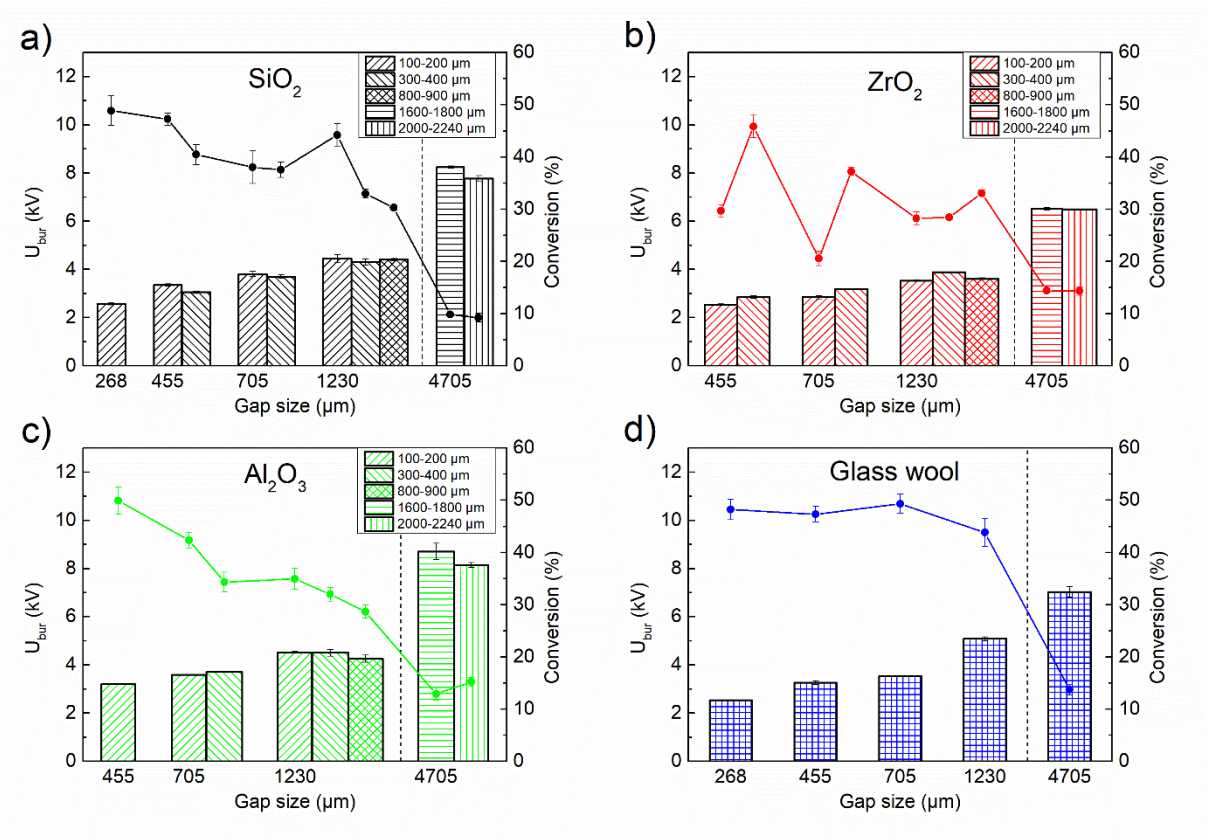

Figure S6: Burning voltage of packed bed DBD (micro) reactors at a constant residence time of 7.5 s. Results are displayed per material type for different sphere sizes (as indicated by the legend) and as a function of gap size, and compared to the conversion of the corresponding packed reactor (solid line).

Finally, the effect of the number of micro discharges can be deduced from Figure S7 and Figure S8. Zirconia gives rise to the highest number of current pulses throughout the whole gap size range Additionally, silica and zirconia tend to give more micro discharges with smaller spheres within a fixed gap size, while alumina does not show this trend. Glass wool shows a steady increase in number of micro discharges with decreasing gap size. Interestingly, the micro discharges all have about the same average delivered charge, independent of the 'material-size-gap' combination.

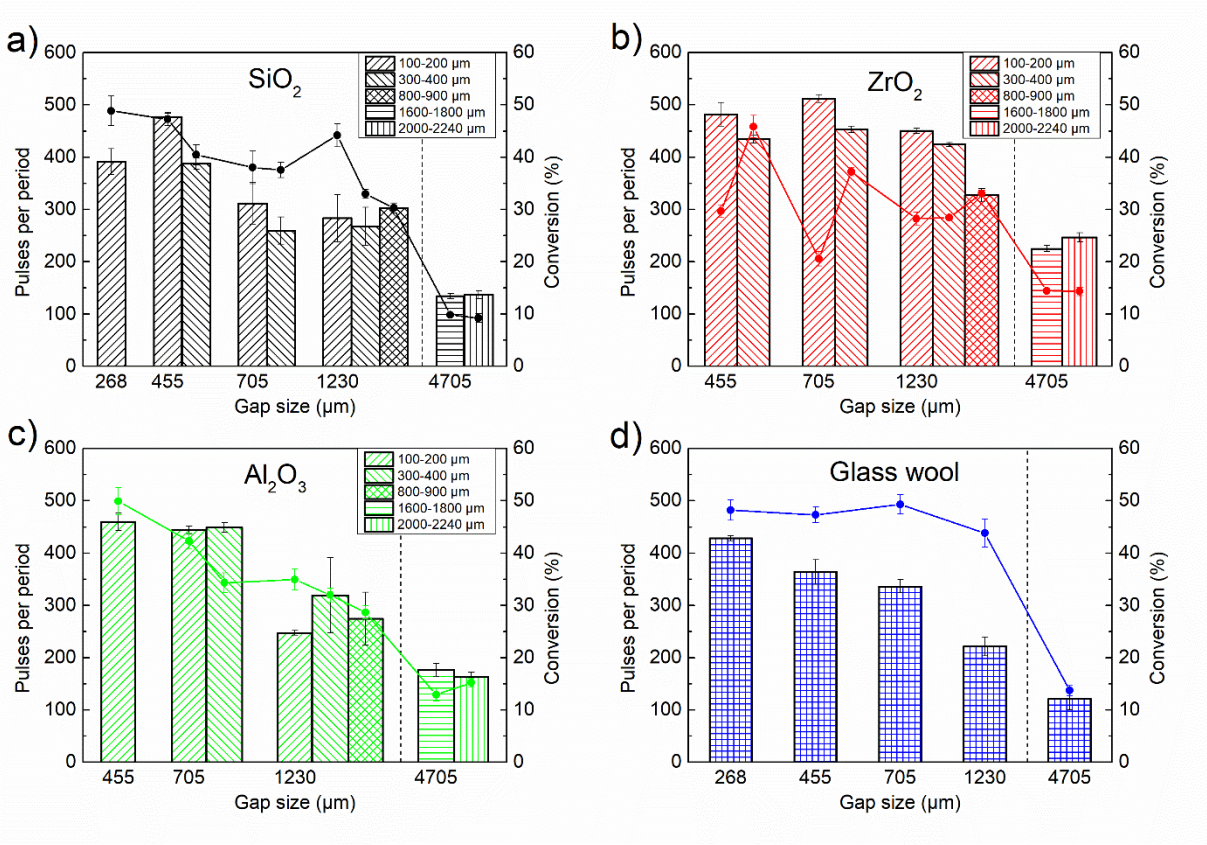

Figure S7: Number of micro discharges in packed bed DBD (micro) reactors at a constant residence time of 7.5 s. Results are displayed per material type for different sphere sizes (as indicated by the legend) and as a function of gap size, and compared to the conversion of the corresponding packed reactor (solid line).

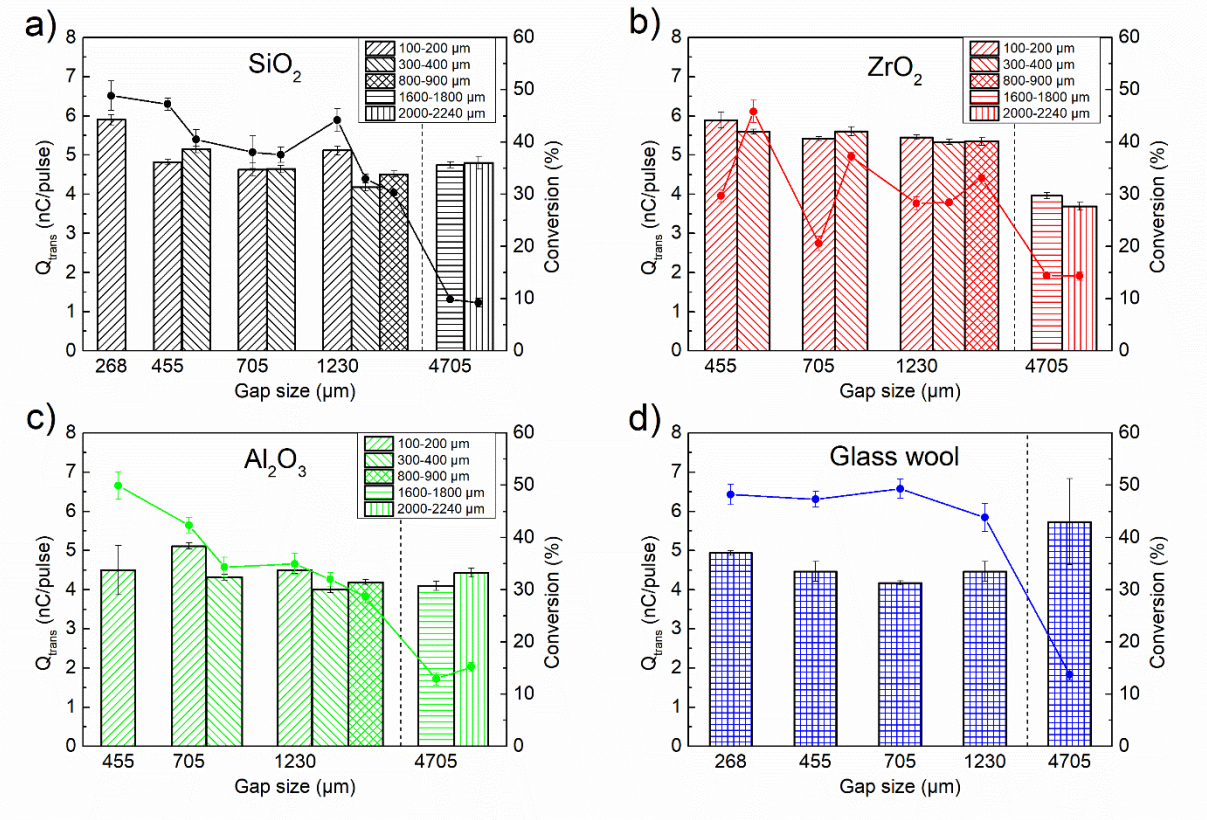

Figure S8: Average displaced charge per micro discharge in packed bed DBD (micro) reactors at a constant residence time of 7.5 s. Results are displayed per material type for different sphere sizes (as indicated by the legend) and as a function of gap size, and compared to the conversion of the corresponding packed reactor (solid line).

References

[1] F.J.J. Peeters, M.C.M. van de Sanden, The influence of partial surface discharging on the electrical characterization of DBDs, Plasma Sources Sci. Technol. 24 (2015) 15016. doi:10.1088/0963-0252/24/1/015016.

[2] T. Butterworth, R. Elder, R. Allen, Effects of particle size on CO_2 reduction and discharge characteristics in a packed bed plasma reactor, Chem. Eng. J. 293 (2016) 55–67. doi:10.1016/j.cej.2016.02.047.